November 2003 • NREL/SR-520-35147

Subcontractor Report

Productivity Enhancement for Manufacturing of Amorphous Silicon PV Modules

Final Technical Report
1 July 2002–30 June 2003

H. Volltrauer
Energy Photovoltaics, Inc.
Lawrenceville, New Jersey

National Renewable Energy Laboratory

1617 Cole Boulevard
Golden, Colorado 80401-3393

NREL is a U.S. Department of Energy Laboratory
Operated by Midwest Research Institute • Battelle

Contract No. DE-AC36-99-GO10337

November 2003 • NREL/SR-520-35147

Productivity Enhancement for Manufacturing of Amorphous Silicon PV Modules

Final Technical Report
1 July 2002–30 June 2003

H. Volltrauer
Energy Photovoltaics, Inc.
Lawrenceville, New Jersey

NREL Technical Monitor: R.L. Mitchell
Prepared under Subcontract No. ZDO-2-30628-14

National Renewable Energy Laboratory

1617 Cole Boulevard
Golden, Colorado 80401-3393

NREL is a U.S. Department of Energy Laboratory
Operated by Midwest Research Institute • Battelle

Contract No. DE-AC36-99-GO10337

NOTICE

Available electronically at http://www.osti.gov/bridge

Available for a processing fee to U.S. Department of Energy and its contractors, in paper, from:

U.S. Department of Energy
Office of Scientific and Technical Information
P.O. Box 62
Oak Ridge, TN 37831-0062
phone: 865.576.8401
fax: 865.576.5728
email: reports@adonis.osti.gov

Available for sale to the public, in paper, from:
U.S. Department of Commerce
National Technical Information Service
5285 Port Royal Road
Springfield, VA 22161
phone: 800.553.6847
fax: 703.605.6900
email: orders@ntis.fedworld.gov
online ordering: http://www.ntis.gov/ordering.htm

Printed on paper containing at least 50% wastepaper, including 20% postconsumer waste

TABLE OF CONTENTS

LIST OF FIGURES

LIST OF TABLES

PREFACE

This draft Annual Technical Progress Report covers work performed at Energy Photovoltaics, Inc. (EPV) under PVMaT contract, Prime Contract No. DE-AC36-99-GO10337, Subcontract No. ZDO-2-30628-14, titled PRODUCTIVITY ENHANCEMENT FOR MANUFACTURING OF AMORPHOUS SILICON PV MODULES. The report covers the period July 1, 2002 to June 30, 2003 of Phase I of the two-year contract.

EPV Contributors to the work are:

David Jackson
Barry Johnson
Joe Stallone
Steve Kane
Zoltan Kiss
Robert Lyndall
Krystyna Szewcsyk
Glenn Zitzer
Hermann Volltrauer
Robert McCort
Anthony Varvar
Kai Jansen
Leon Chen
Yuan-Min Li
Alva Sizemore
Bogulawa Wierzbowicz
Alan Delahoy

SUMMARY

During Phase I, EPV conducted parallel research efforts for achieving higher stabilized module power output through improvements in several manufacturing processing steps, with particular emphasis on the thin-film deposition process. The dual goals of achieving a 10% gain in stabilized output, and a 20% reduction in direct costs were accomplished. Early in Phase I, a thorough evaluation of single junction and tandem amorphous silicon (a-Si) modules was carried out with the goal of determining the best option to use (as a function of application) based upon EPV's proprietary batch deposition process. The analysis considered total energy delivery over realistic conditions and the impact on equipment needs and production costs. EPV has concluded that the tandem process is more appropriate for its needs at this time.

OBJECTIVE

The overall objective of this subcontract over its two-year duration is to continue the advancement of EPV's a-Si production manufacturing technology and improve the production equipment used in manufacturing. This will allow EPV to reduce module costs by increasing module output, throughput, and yield.

3.1 TASK 1: PRODUCTIVITY IMPROVEMENT – I

The objective of Task I was to compare the benefits of manufacturing single junction and tandem a-Si modules, combine or eliminate process steps, increase the throughput of the deposition system by 20%, and reduce both labor and material costs. In this phase, a study was carried out to select process steps to automate in Phase 2, and one RF matching network was automated.

M-1.1.1 Complete Comparison of Benefits of Manufacturing Single Junction and Tandem a-Si Devices

The analysis of single junction and tandem modules was divided into manufacturing or cost related issues, and quality issues. A third point for analysis was the change in relative advantage of both types of modules, resulting from improvements that are planned under this contract for the near future. These considerations are discussed below.

A. Manufacturing and Cost Related Issues

1. The complete a-Si deposition cycle time for single junction modules is approximately 70% of the tandem cycle time. A relative manufacturing cost savings will be realized when manufacturing single junction modules, because a shorter cycle time will result in reduced labor, electricity use, gas consumption, liquid nitrogen use, and gas scrubber costs.
2. In principle, less deposition equipment is required for single junction modules. For example, the EPV batch process for a 5 MW per year tandem junction facility requires two deposition systems. With a fairly modest reduction in deposition cycle time for single junctions, to slightly under 2.5 hours, only one deposition system with all the associated components is required for a 5 MW per year facility. This represents a considerable savings in equipment costs.
3. Lower laser costs for tandems partially offsets their higher deposition system costs. About one-half of the number of laser scribes is required for a tandem module compared to a single junction module; therefore, tandem module manufacturing facilities require fewer lasers per scribe station and reduces equipment cost.
4. In full-plate shuntbusting (see M-1.3.1 below), shorts are cured (or "burned out") by discharging a capacitor through the plate as part of the IV Testing procedure. This full-plate shuntbusting is not as effective for single junction plates (much higher currents must be passed to generate voltages similar to those developed on tandem plates); therefore, a separate shuntbust station would be required for single junction facilities.

   Cost Comparison - Our silicon deposition process for tandems currently requires about 4.5 hours from door closing for one run to door closing for the next. For a tandem module facility with a 5 MW per year capacity, two complete deposition systems with preheat and cool down chambers are required. Table 1 lists the time available per single junction deposition run using one deposition system for a 5 MW per year operation and taking into account the length of the workweek and yield.

Table 1: Deposition Cycle Time for Single Junction Operation

Operation	80% Overall Yield	90% Overall Yield
5 day/wk	1.84 hrs	2.07 hrs
6 day/wk	2.21 hrs	2.49 hrs

Based on several tests carried out during the past year (see M-1.2.1 below), the 2.49 hours is very likely achievable with a single deposition system when making single junction devices. Even the 2.21 hours is within reach (in cycle time reduction tests with tandems the shortest deposition cycle time achieved by EPV was about 3.5 hours). Considerable cost savings can be realized when building a factory that makes single junction modules compared to tandems. Material and electricity costs are also impacted. The costs will be looked at from the point of view of changing to single junction modules from tandems.

Equipment – To increase the capacity of a 2.5 MW per year tandem operation to a 5 MW per year single junction operation, an extra laser and associated optics has to be added to the three laser stations (one IR and two green), and a shuntbust station is required. This upgrade would cost approximately 7% of the total equipment cost of the 2.5 MW per year tandem facility. To upgrade a tandem line from 2.5 MW per year to 5 MW per year, a second deposition system is required. This upgrade would cost approximately 20% of the equipment cost of the 2.5 MW per year tandem facility. An approximately net 13% equipment cost saving can be realized when increasing the capacity of a 2.5 MW per year tandem operation to a 5 MW single junction process compared to a tandem process.

Material – Depositions for single junctions will be slightly shorter, mainly due to shorter gas stabilization times. Less gas, fewer scrubber cartridges, and less liquid nitrogen will be used, for a total saving of approximately 4% in material costs. The LED arrays for the lasers will be used less with tandems and thus increase material costs for single junction by approximately 1%. The net advantage for material costs for single junction modules is approximately 3%.

Labor – No significant difference in labor costs exists between the two types of modules. The labor savings realized for the deposition system is mostly offset by the need to do shuntbusting for single junction modules.

Electricity – Because of the shorter a-Si deposition times, an estimated 7% of electricity cost is saved with the single junction process; this amounts to an approximate savings of 0.4% in material costs.

B. Quality Related Issues

1. Stabilized Output - A complicating factor in comparing modules made at different times, and light soaked at different times and for different durations are the seasonal effects that influence both single junction and tandem modules.

   Light soak data is only available for the older runs that do not have the increased active area. This data, as well as data for comparable single junction runs, will be discussed. Averaged data from four tandem runs (all measured at the same time) will be compared to calculated values obtained from a model. The same will be

done with data from three single junction runs (also measured at the same time). Data is averaged because the process as well as power output differences between runs is relatively small and long-term variations are likely to be similar for a given type of module. When our measurements extend to longer durations, differences between modules and runs might be revealed.

It is well known that seasonal fluctuations in a-Si modules exist, although the magnitude can vary from module to module, especially between single junction and tandem (and with locations and climate). It is also believed that there is a long-term downward trend in output in addition to the seasonal fluctuations. The magnitude of the long-term trend is even more difficult to determine quantitatively, since it is a long-term effect and small on a yearly basis. Nevertheless, we do have enough information to estimate the seasonal variations and (less well) the longer-term effects by fitting the data to a model. The model used in this study is from Muirhead et al. [1]. It is assumed that both seasonal variations and long term degradation are the same for all tandems and single junction modules for this analysis.

The analysis consists of fitting the averaged data to the model by adjusting the input parameters for the best "eye-ball" fit to the data. The calculated values are extended to a 500 day period to show the seasonal variations that might be expected. The equation used to represent the long-term behavior of the modules is the following:

$$P=A*(1+B*\sin(2*Pi*(t/365.25)+C)-D*\ln(t+E))$$

In this equation,

P = power (W)
t = time (days)
A = (together with ln(E)) the power measured when the module is first placed outside (W)
B = magnitude of the seasonal variations (number)
C= phase factor which takes into account the time of year when light soaking was started (days)
D = long term loss term (number)
E = time related term that describes the initial rapid drop.

The measured averages and calculated values for power output of the modules are shown in Figures. 1 and 2.

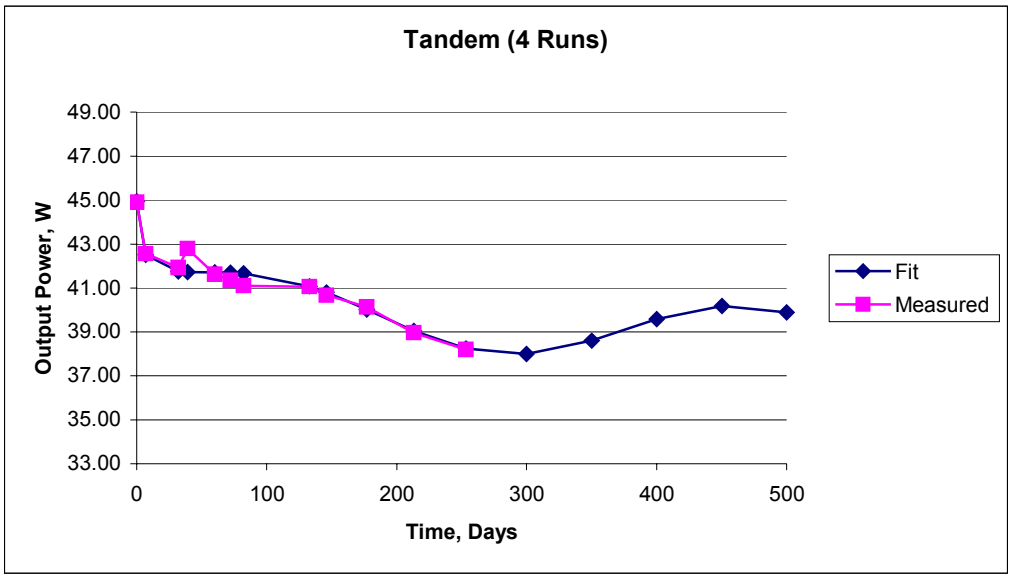

Figure 1: Long Term Performance for Tandem Modules

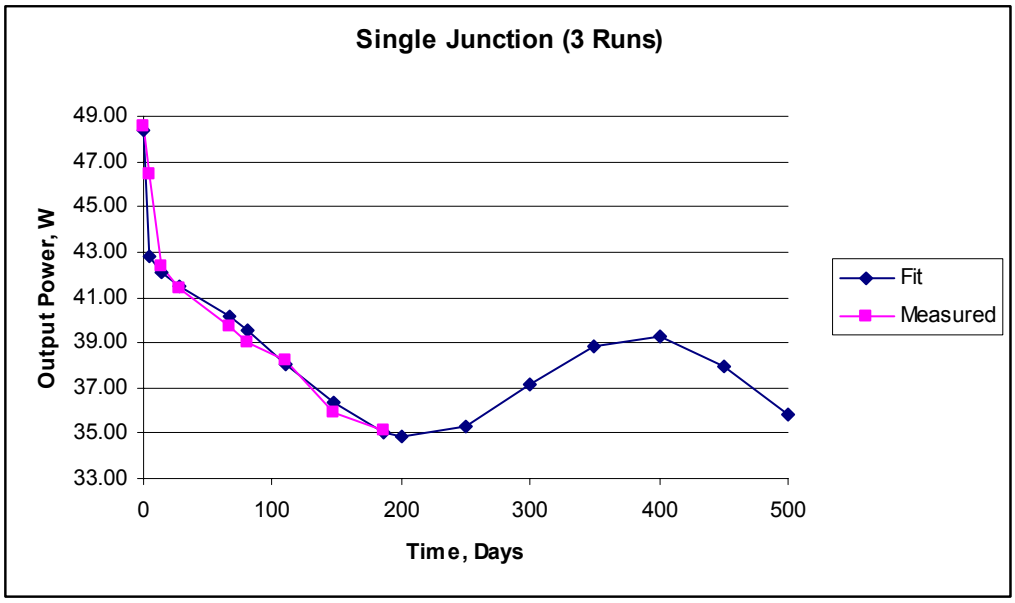

Figure 2: Long Term Performance of Single Junction Modules

The last five measurements were made outdoors for both graphs. Since neither of these groups of modules have the new laser pattern with tighter scribe alignment, a modest (see M-1.2.3 below for an analysis of active area) 4% higher output is expected for the tandem and 8% for single junction. Adding these amounts, the values given in Table 2 for one year and twenty year power outputs were calculated. The seasonal and long-term degradation terms used in the calculation are also shown.

Table 2: Comparison of Single Junction and Tandem Long Term Performance

Type	B (Seasonal)	D (Long-Term)	Long-Term Output	
			1 Yr.	20 Yrs.
Tandem	.032	.020	40.6 W	37.9 W
Single Junction	.060	.023	39.9 W	36.7 W

In real applications, somewhat higher outputs are likely to be obtained because the modules would be under load, whereas in these tests the modules were in an open circuit condition. In real applications, somewhat higher outputs are likely to be obtained because the modules would be under load, whereas in these tests the modules were in an open circuit condition.

2. Energy Delivery - The total energy delivery for single junction modules appears to be higher than for tandems (both having the same power rating). This conclusion is based on three types of tests that have been carried out to quantify this comparison. Observed differences vary depending on the type of test and weather conditions. Figure 3 shows the results of one test (which is typical, in general appearance, of all three) in which the relative gain in integrated energy delivery of a single junction module over a tandem is plotted over the course of a day. The data was obtained by exposing four light-soaked modules (two single junction and two tandems) to sunlight, while operating them at their indoor-measured maximum power voltage (Vmp) using a constant voltage load circuit. The energy output from the two pairs of the same type of modules was averaged and the data was plotted as gain of a single junction module relative to a tandem.

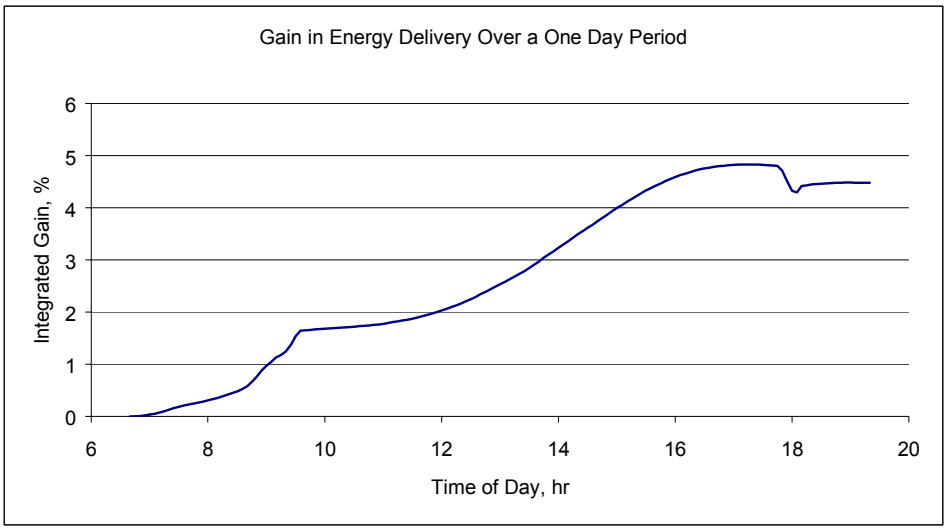

Figure 3: Gain in Energy Delivery of Single Junction Over Tandem at STC Vmp

The rapid early rise in the morning is partly due to the lower current tandems typically produced during this time (accentuated by the constant voltage circuit used). The small drop near 18 hours is due to earlier shading of one of the single junction modules, which was corrected for subsequent tests.

When the output is normalized to the peak value at approximately noon, differences between single junction and tandems become essentially zero for this test (at Vmp). However, measuring only Isc for the same four modules and normalizing this current with the noon peak again results in a roughly 2% higher output for the single junction modules as shown in Figure 4.

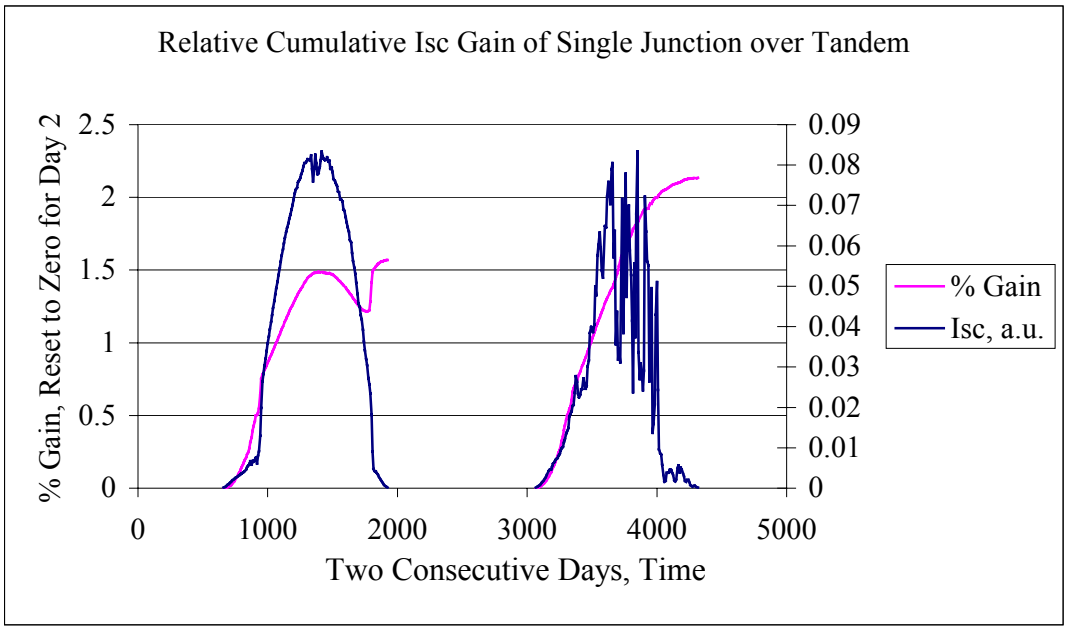

Figure 4: Gain in Energy Delivery of Single Junction Over Tandem at STC Vmp for Sunny and Cloudy Day

Another set of tests similar to the two described above was carried out with the operating voltage set at 28 V; the typical Vmp of our modules is slightly over 40 V. The same four modules were monitored for 7 days. During this time the average difference in output between the single junction and the tandem varied between 1.8% and 4.4%, averaging slightly over 3.4%. The summary of these tests is provided in Table 3.

Table 3: Summary of Energy Gain of Single Junction Compared to Tandems

Load Voltage	**Normalized at**	**Duration (days)**	**Average % Gain for Single Junction**	
			P (W)	**Isc (A)**
Vmp (STC)	P@Vmp (STC)	2	5.1	-
Vmp(STC)	P (noon sun)	2	0.5	-
0 V (at Isc)	Isc (noon sun)	2	-	2.3
28 V	P (noon sun)	7	3.4	-

In all cases, sunny days tend to result in smaller differences while cloudy days give the higher values (as shown in the figure above).

3. Other Factors

   a. Because fewer layers are needed to make single junction modules, matching the layers' thickness should not be as critical for single junction as for tandem modules. Thickness uniformity should also not be as critical for single junction modules.

   b. The IV Tester flash lamps' spectral output quality is not as critical for single junction as it is for tandems.

   c. For a given module area, tandems have a larger active area, because there are fewer cells and hence scribes. Prior to the new layout of the laser patterns, tandems had a 5 to 6% dead area attributed to scribes, compared to over a 10% loss for single junction modules (with the use of a single xy table for scribing all three films, these numbers become a 1.5% loss for tandems and 3% for single junction modules).

C. Performance Summary

Three comparisons have been made between single junction and the tandems. The most important is the stabilized output of the modules. Our light soak module data for recent recipes are only about 10 months old, but using a mathematical model to represent seasonal variations, reasonable comparisons between single junction and tandem modules can be made. Allowing for tight scribe alignment, tandem outperform single junction modules by about 3%.

The second comparison, of energy delivery, favors single junction modules. The above data suggests that single junction modules deliver between 2-3 % more energy than tandems, depending on the weather and the type of test.

Energy delivery is based on the output of the module. With the tandem providing approximately 3% more power output under standard test conditions and the single junction having a relative 2-3% greater energy delivery, the two types of modules provide about the same energy in real life. A third, but unknown, factor consists of the gains that we expect to achieve (as part of this contract) in the near future. Active area gains have already been included in the power output comparisons above, leaving the issue essentially at a draw. One area where improvements might be realized in tandems compared to single junction modules is in achieving better uniformity. Since tandems suffer more from non-uniformity and perform roughly equivalent to single junctions, the existing non-uniformities, if improved on, will benefit tandems most.

A cost related issue, yield, may be different for the two types of devices. No quantitative analysis can be applied at this time, although the higher complexity of making tandem depositions might result in a lower yield. This might be partially offset by the higher complexity of laser scribing single junction modules, but laser scribing is still simpler than current tandem deposition techniques, and therefore one would expect that the yield for single junction modules might be higher.

D. Status

EPV's standard process is for tandem modules. For existing factories, there is a net equipment cost associated with changing from tandems to single junction because of the additional lasers that would be required. The deposition equipment already exists; hence no saving in this area is possible unless the capacity was increased. The material cost savings alone does not justify changing to single junction, because of the risk that the above uncertainties entail.

The situation may be different for new 5 MW per year factories where a net 12.5% equipment cost savings can be realized for a single junction operation compared to a tandem. This, together with the lower production costs and essentially equivalent performance, makes the single junction module look attractive, although more reliable and longer-term test data under more varied conditions than we have been able to provide are needed to form a conclusion. When we start applying a ZnO/Al back contact on large modules during Phase II, we may find differences in the gains between single junction and tandems that could influence our decision for future manufacturing facilities.

M-1.1.2 Eliminate Need for Masking Plates During Edge Film Removal

In early work, lasers were used to edge isolate the thin films from the edge of the plate. This process is clean, but the equipment is expensive compared to the equipment needed in the sandblasting process. In addition, the initial leakage tests for the lasered modules were spotty, and the appearance was deemed unacceptable. The sandblasting process is quicker and exceeds the electrical isolation test requirements. The sandblasted edge around the perimeter of the module also gives it an attractive "frame" effect.

This task had two objectives. In addition to eliminating the need for masking the PV plate during our sandblasting process (for cost saving reasons), an equally important objective was to minimize the thin-film area that is damaged during sandblasting.

Masking of the plate prior to sandblasting was done because the sandblasting process generated dust and debris that was difficult to remove from the plate. A benefit of the masking was that the edge of the sandblast region was well defined. The downside of it was that it was a very labor-intensive, manual procedure. To eliminate masking, the sandblasting process had to be improved, both to better define the region sandblasted and to make it a cleaner process. These objectives were met with a new prototype single-head sandblaster. By changing the vacuum pickup system, debris was efficiently removed. In addition, the static discharge system added to the machine prevented blasted debris from gravitating to the surface of the glass. Precisely directed air jets in the blasting area helped direct the debris into the pickup and also resulted in the required sharp dividing line between the sandblasted region and the film.

To determine how well defined the sandblasting boundary is, the distance from the sandblast edge beyond which no damage is caused was determined. This was done with a specially prepared small plate in which the aluminum film adjacent to the sandblast edge was removed in steps (this is accomplished by sputtering with a mask) and the shunt resistance of the resulting cell measured. The results of such a test are shown on the graph below. Shunt resistance was measured (readings higher than full scale at 200 ohms are taken to be 200 ohms) between two adjacent cells and the distance was measured from the edge of the plate to the beginning of the aluminum film. The sandblasting

removed 0.375 inches of thin films around the perimeter of the plate. Figure 5 shows that significant damage stops shortly after 0.375 inch.

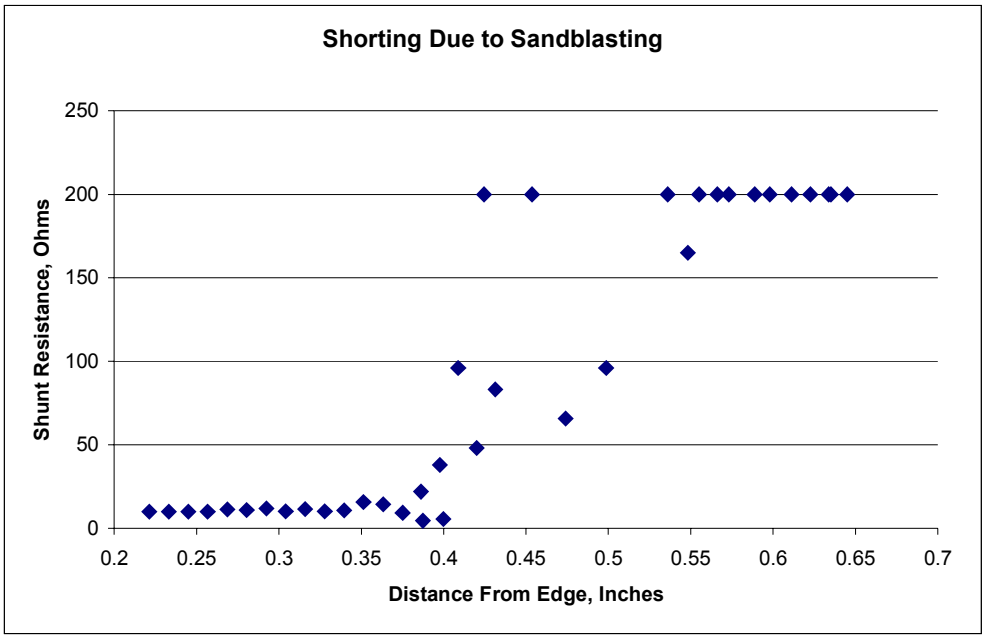

Figure 5: Damage Caused by Sandblasting

In addition to providing a sharply defined sandblast area, the modules easily passed the leakage test at 2.5 times the system voltage plus 1,000V (i.e. 2,500VDC).

The cost savings resulting from avoiding the masking and combining the laser isolation step with the initial tin oxide lasering, amounts to an approximately 9% reduction in direct labor costs. This reduction is the combined time of masking the plate with paper, removing the paper, cleaning, and transporting the plate to the stations involved.

M-1.2.1 - Complete a 20% Reduction in the a-Si Deposition Cycle Time for Tandem Devices

Our current cycle time for tandem runs is approximately 4.8 hours. Both preheat and cool-down times are shorter than this. Approximately 3.6 hours of the 4.8 hour cycle time are used for pumping down the system, mostly in the hi-vac mode. Six deposition runs have been made with variations to this pump-down sequence, each with reduced pump down times. The extended hi-vac pumping sequence normally used for the initial pump down from atmospheric pressure and between the p and i-layers was replaced with a preset relatively short time period of rough pumping, followed by backfilling the chamber with hydrogen, and quickly pumping the chamber to some intermediate pressure.

Both single and tandem junction runs were made with the modified pump down sequence. With the deposition times being the same for the comparisons, the total times from door closing to venting are provided in Table 4.

Table 4: Cycle Time Reduction for Single Junction and Tandem Runs

Type	Standard Process (Hrs)	Reduced Cycle Time (Hrs)
Single Junction	3.4	2.5
Tandem Junction	4.8	3.6

In both cases the cycle time reduction amounted to approximately 30%. The initial power output from the reduced cycle time plates was essentially the same as the power output from plates made with the standard process.

Because comparisons between different deposition runs have some uncertainty associated with them, and changes in stability resulting from different pump down methods might be small, a deposition run was made in which two variations of the pump down sequence for the initial pump down, and three variations for the pump down between the p and i-layers were carried out (in the same run). Data for only this run will be reported. A single junction run was chosen, because compared to a tandem run, there are fewer pump downs and the degradation is greater than it is for tandems, making module stability differences easier to detect.

The procedure for this run, was to use a short 20 minute pumping sequence for the initial pump down (compared to the standard 50 minutes) followed by depositing p-layers on twelve plates in three RF sections. Next, the system was pumped down using the standard procedure (with the 50-minute pump down), and p-layers were deposited in three additional sections. With these two variations of the initial pump down, three pumping variations were then used between the p and i-layers each one with a RF section that had a short initial pump down and one with a long initial pump down. Averaged initial results for the six variations of this run are shown in the Table 5.

Table 5: Initial Electrical Parameters for Pump Down Variations

RF Section	Initial Pump Down (min)	p to i Pump Down (min)	Voc (V)	Isc (A)	FF (%)	P (W)
4	20	20	59.2	1.059	70.1	43.9
5	20	40	59.6	1.068	68.0	43.3
6	20	50	59.6	1.083	67.7	43.7
7	50	20	59.4	1.084	67.7	43.6
8	50	40	59.2	1.082	68.6	43.9
9	50	50	58.8	1.083	68.6	43.7

Within the precision of the measurements, the parameters for all six variations are essentially the same. The only possible trend pertains to the three short initial pump downs, in which Isc increases and FF decreases as the p to i pump down time is increased. This "trend" is very likely due to measurement uncertainty, since the opposite is expected for FF.

To determine the stability of the plates, two light soaking studies were carried out: 1) accelerated light soaking and 2) outdoor exposure. The same plates were used for both

studies. One plate from each of the six pump-down variations was cut into three sections - one 3 inch wide section from the center, and two 23 inch wide sections from the two sides. The two larger plates were made into "half-modules" and a 3x3 inch piece was cut from the center section. Small, isolated devices (dots) were made on each 3x3 inch piece. The "half-modules" were light soaked outside, while the dots were subjected to Accelerated Light Soaking (ALS) at approximately 47 suns for 162 seconds. While ALS does not predict the module's stabilized performance, it can reveal differences in stability between different devices.

Table 6 compares the electrical parameters for the dots of the six cut plates subjected to ALS at 0 and 162 second; as well as, their percentage changes.

Table 6: Electrical Parameters of ALS Dots for Pump Down Variations

Pump Down		Voc (mV)			Isc (mA)			FF(%)			Efficiency (%)		
Initial (min)	p to i (min)	at Time,sec		Change	at Time, sec		Change	at Time,sec		Change	at Time, sec		Change
		0	162	%	0	162	%	0	162	%	0	162	%
20	20	778	802	3.1	12.3	11.2	-8.8	72.7	55.5	-23.7	6.93	4.97	-28.3
20	40	779	805	3.3	12.2	11.1	-8.9	71.6	55.5	-22.6	6.81	4.96	-27.1
20	50	784	806	2.8	12.7	11.3	-11.5	70.3	54.1	-23.0	7.02	4.92	-29.9
50	20	779	804	3.2	12.7	11.3	-11.3	70.1	53.9	-23.2	6.96	4.90	-29.6
50	40	779	798	2.5	12.6	11.2	-10.6	71.3	53.9	-24.4	6.99	4.84	-30.8
50	50	778	798	2.5	12.6	11.4	-9.3	72.4	55.3	-23.7	7.09	5.03	-29.0

No real trends are apparent. The results shown in Table 7 were obtained for the half modules light soaked outside.

Table 7: Electrical Parameters of Light Soaked Half Modules for Pump Down Variations

Pump Down		Voc (V)			Isc (A)			FF (%)			Efficiency (%)		
Initial	p to i	at Time, days		change	at Time, days		Change	at Time, days		Change	at Time, days		Change
min	min	0	35	%	0	35	%	0	35	%	0	35	%
20	20	58.9	61.4	4.3	483	419	-13.3	69.2	57.5	-17.0	19.7	14.8	-25.0
20	40	59.0	60.9	3.3	482	408	-15.4	65.2	59.2	-9.2	18.5	14.7	-20.7
20	50	59.8	61.8	3.3	494	439	-11.3	66.0	57.6	-12.7	19.5	15.6	-20.0
50	20	59.5	61.4	3.2	492	433	-11.9	66.4	56.7	-14.5	19.4	15.1	-22.3
50	40	59.2	61.1	3.3	495	433	-12.4	67.4	57.1	-15.2	19.7	15.1	-23.3
50	50	59.0	60.6	2.7	495	437	-11.5	68.3	57.9	-15.1	19.9	15.3	-22.9

As is the case with ALS, no real trends are apparent. At this point it can be concluded that the shortened pumpdown used in these runs does not have any significant deleterious effect on module performance and a 20% cycle time reduction has been achieved.

M-1.2.2 – Complete Development of First Version of Automated Batch Run Analysis

The reason for developing an automated batch run analysis is two-fold. The first is to collect any insight that has collectively been acquired over the years into an evaluation of runs. The second applies to a factory where as many as a dozen runs may be made in a

single day and early identification of a problem is important. The intention of the analysis is to have a concise summary of a run that has enough information to not only inform the manager of any problems but also identify their probable cause.

Several problems will be highlighted in the analysis report below. Following a discussion of the analysis approach, tests designed to provide input on the cause of shorts will be discussed.

All data used in this first version of the automated run analysis program were generated by the IV tester. Other input that is now available from manual measurements will be included when more of the equipment is connected to the network.

Because most runs do not have any "problem" plates, a composite run was assembled that included "problem" plates to illustrate how problem plates are identified and classified. Plates are considered "problem" plates if their output is less than 90% of the run average. After these "problem" plates are eliminated from the run, the average is re-calculated and possibly more plates removed. For the analysis presented below, a full, forty-eight plate run was created from four separate partial runs, each contributing 12 plates.

The information provided in the automated run analysis program includes two summary tables. Table 8 shows the electrical parameters for all plates and Table 9 shows averages for each RF section in the deposition system. Two graphs are also included. Figure 6 shows the output power for each plate and the change after heat aging, and Figure 7 shows the relationship between low light level Voc and FF. A list of problem plates with possible causes is generated from a lookup table, which is summarized and presented together with the other data in Table 10.

A. Analysis for Run

1. Averages for All Plates – In addition to Voc, Isc, FF and Power, the series resistance (Rs), shunt resistance (Rsh) and (LLLVoc) are also shown. Plates 1-12 are from run 242, 13-24 from run 231, 25-36 from run 239 and 37-48 from run 238.

Table 8: Electrical Parameters for Composite Run

Composite run			Deposition: 11/11/02		System A	Box Carrier-A	
Plate #	Voc (V)	Isc (A)	FF(%)	P (W)	Rs	Rsh	LLLVoc (V)
1	58.7	1.133	67.4	44.8	8.5	14384	37.2
2	59.2	1.192	66.6	47	8.7	6048	30.8
3	59.8	1.177	65.6	46.2	9	3381	28.8
4	59.2	1.187	66.4	46.7	9.1	3585	28.8
5	59.1	1.114	69	45.4	9.4	5000	36.6
6	59.2	1.181	63.8	44.6	9.9	1983	18.8
7	59.8	1.175	67.7	47.6	9.9	10449	35.4
8	60.4	1.114	68	45.8	8.7	14364	38.4
9	59.8	1.12	68.3	45.7	9.2	28724	37.1
10	59.2	1.169	64.9	44.9	10	7666	31.8
11	59.2	1.19	66.7	47	9.2	7671	28.1
12	59.2	1.108	69.5	45.6	9.3	3283	36.1
13	59.6	1.251	65.5	48.8	9.1	3026	26.4
14	58.6	1.236	64.1	46.4	9.4	3822	18.4
15	59.3	1.216	66.3	47.8	9.8	57383	29.7
16	59.8	1.204	67	48.3	10.1	8215	29.2
17	59.8	1.208	67.4	48.7	10	28699	28
18	59.9	1.202	67.7	48.7	10.1	3959	33.8
19	59.3	1.196	67.9	48.2	10.2	5466	33.3
20	59.3	1.215	66.8	48.1	9.7	6047	28.6
21	59.3	1.227	65.7	47.8	9.7	10436	30.1
22	59.3	1.152	68.2	46.6	9.6	2209	37
23	59.4	1.156	64.1	44	10.6	7179	39.2
24	56.3	1.139	53	34	11.4	309	9.8
25	57.5	1.176	60.6	41	9.2	2797	31.4
26	57.7	1.199	64.3	44.5	9.7	3827	30
27	58.2	1.165	62.1	42.1	9.3	4592	28.9
28	58.2	1.161	62.5	42.3	10.7	8829	30.6
29	58.3	1.17	59.2	40.3	10.9	1822	34.3
30	57.6	1.178	57	38.7	11.7	1161	35.1
31	58.4	1.15	58.5	39.3	12.2	2494	38.3
32	57.7	1.14	43.8	28.8	23.7	197	41.2
33	57.7	1.142	46.6	30.7	20.8	347	34.3
34	56.6	1.113	43.2	27.2	22.1	200	35.9
35	56.6	1.06	36.9	22.2	27.7	114	39.6
36	57.2	0.754	33	14.2	36.8	110	35.3
37	59.1	1.153	61.4	41.8	8.6	5744	34.6
38	59.1	1.141	66.1	44.6	8.6	23010	36.4
39	59.1	1.123	63.6	42.2	10	3484	40.8
40	59	1.133	61.7	41.3	10.2	3029	41.2
41	59.1	1.149	64	43.5	9.4	57522	40.2
42	59	1.147	62.9	42.6	8.6	115125	39.3
43	59.1	1.149	61.4	41.7	9.8	7197	38.3
44	59.1	1.153	64.4	43.9	8.8	3594	37.7
45	59	1.145	61.6	41.6	8.8	6766	37.7
46	56.7	1.137	57.1	36.8	15.5	792	36.1
47	57.3	1.133	58	37.7	14.8	1646	39
48	57.3	1.123	57.4	36.9	15.6	1824	40.1

2. Averages for Each of the Twelve RF Sections

Table 9: Electrical Parameters for Composite Run Averaged by RF Section

Averages by RF Section							
RF section	**Voc**	**Isc**	**FF**	**P**	**Rs**	**Rsh**	**LLLVoc**
1	59.2	1.172	66.5	46.2	8.8	6850	31.4
2	59.6	1.146	67.1	45.8	9.5	7949	32.3
3	59.3	1.147	67.4	45.8	9.4	11836	33.3
4	59.4	1.227	65.7	47.8	9.6	18112	25.9
5	59.6	1.205	67.5	48.4	10.0	11043	30.9
6	58.6	1.169	62.8	43.1	10.3	5033	29.0
7	57.9	1.175	62.4	42.5	9.7	5011	30.2
8	58.0	1.160	54.6	36.8	14.6	1419	37.2
9	57.0	1.017	39.9	23.6	26.9	193	36.3
10	59.1	1.138	63.2	42.5	9.4	8817	38.3
11	59.0	1.150	63.2	42.9	9.2	45859	38.9
12	57.6	1.135	58.5	38.3	13.7	2757	38.2

3. Graphs – The graph in Figure 6 shows the output power of the plates before and after heat aging and the ratio of after to before. The second graph shows the relationship between LLLVoc (shunting) and FF.

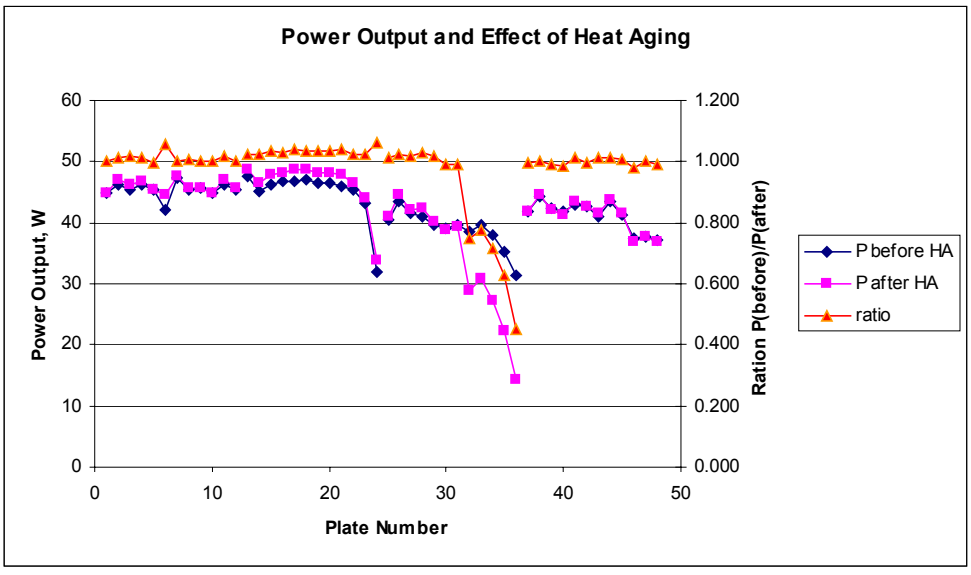

Figure 6: Effect of Heat Aging Composite Run

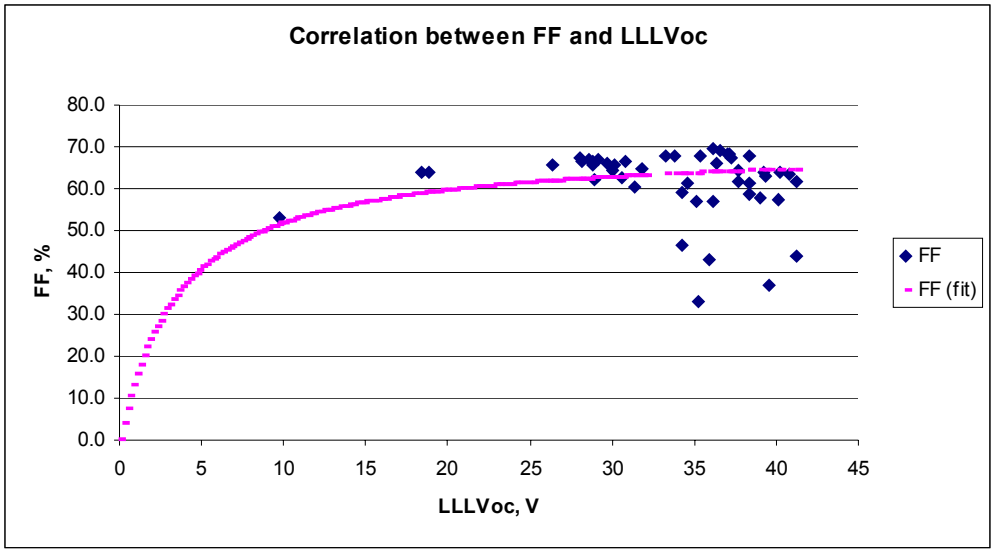

Figure 7: Relationship Between FF and LLLVoc for Composite Run

4. Problem Plates – Table 10 lists plates whose output was more than 10% below the run average. BHA is before heat-age and AHA is after heat-age.

Table 10: Summary of Problem Plates for Composite Run

Plate	Output Relative to Average	Heat-age Ratio A/B	Possible Problem
24	0.794	1.062	shorts, aluminum scribing
32	0.700	0.748	sputtering - check order in which plates were sputtered
33	0.745	0.777	sputtering - check order in which plates were sputtered
34	0.661	0.716	sputtering - check order in which plates were sputtered
35	0.539	0.627	sputtering - check order in which plates were sputtered
36	0.346	0.452	sputtering - check order in which plates were sputtered
46	0.865	0.980	lasering - look for cross scribes, incomplete silicon lasering,
47	0.885	1.000	lasering - look for cross scribes, incomplete silicon lasering
48	0.867	0.991	lasering - look for cross scribes, incomplete silicon lasering

As mentioned, the potential problems are obtained from a lookup table. The logic for the assignment of problems is as follows (using the plates from this composite run as examples):

Plate 24 – This plate initially has low power output but this increases significantly after heat aging. This indicates shorts, at least some of which are likely to be due to aluminum scribing problems. Because this is the only plate within an RF section of the run with low power output, particulates from the deposition system are unlikely to be the cause of the problem.

Plates 32 through 36 – The drop of power output resulting from heat aging indicates poor contact between the silicon and aluminum. Other plates in the run that did not decrease after heat aging might also have been affected by this problem but to a lesser extent. Typically these problems occur on several plates that are sputtered consecutively. Note that the graph in Figure 7 of LLLVoc and FF shows these plates fall well below the average line for the other plates. The points on the smooth line are fit with the equation FF = 70*LLLVoc/(LLLVoc+3.5). This type of fit was found to describe the relationship of FF with LLLVoc when significant shunting occurs and has no other significance.

Plates 46 through 48 – because these plates do not drop after heat aging, and do not have low shunt resistance, the problem is likely due to a high series resistance from either incomplete scribing of the silicon, or more likely crossing scribes. Damage to the tin oxide from too vigorous scribing with the green laser is unlikely because of the limited power of this laser under the conditions used.

The 4-5% higher Isc for sections four and five should also be highlighted because such large variations should not occur.

Shorts - Shorts have always been a problem. Every plate is electrically shorted to some degree. Some cells are moderately or badly shorted, while others are hardly shorted at all. Even badly shorted cells are usually able to contribute some output because of the length of the cell. With the end-to-end aluminum resistance along a single segment being close to 50 ohms, even a dead short at one end will only loose about one fourth of the output of that cell.

Shorts between cells may be caused by the following:

1. incomplete tin-oxide scribing,
2. incomplete aluminum scribing, or
3. pin-holes in the a-Si that result in shorts when the aluminum is sputtered

We estimate that between 2 - 5% of the module output is lost due to shorts. A test was completed to determine the relative importance of the three problems listed above, since knowing their cause would make it easier to reduce the shorts.

To assign shorts to specific causes, shunt resistances were measured on the 40 cells of a plate after tin-oxide scribing. Some cells were slightly shorted (resistances in the kiloohm range). However, measuring shunt resistances after completely processing the plates did not show any correlation with the tin-oxide

shorted cells. Based on this limited but convincing evidence, it is likely that tin-oxide shorts do not play an important role in module output losses.

The second source of shorts was investigated by re-scribing an already scribed plate. We assumed that if aluminum is shorting some cells, then after the second scribing the shunt resistances of some of the cells will decrease, while others might increase. If aluminum lasering is an important contributor to shorts, we would expect to see new patterns of shorts develop on a plate after a second scribe.

In this test, shunt resistances (the average of measurements at the two ends and the middle) of 4 cells out of 40 decreased by approximately a factor of two or more, while 15 others increased by a factor of two or more. The fact that 19 of the 40 cells had dramatic changes supports the proposition that lasering is a source of shorts. It was also found that the cells with shunt resistance less than about 70 ohms (6 out of 40), did not change (within the measurement repeatability of approximately 10%) after lasering. This suggests that these cells were shorted for reasons other than poor aluminum scribing. Since we did not see any significant correlation between tin oxide shorts and final shorts, a likely cause of these shorts is probably an aluminum to tin oxide contact through the silicon, possibly from a pinhole.

M-1.3.1 - Reduce Labor Costs by Eliminating or Combining Process Steps

Two process steps were considered candidates for elimination or folding into other steps, heat-aging and shuntbusting. An argument can be made that the former can be done on a sampling basis (if at all) rather than for all plates, and the latter can be made part of the IV test procedure where it requires no additional labor to carry out.

A. Heat-Aging

Our current process includes a heat-aging step in which the plates are brought to 150^0 C and held for one hour. This step serves two purposes. First, it is a quality control (QC) test that is intended to verify that the internal tin oxide to aluminum contacts are good, and second, it typically results in a few percent increase in power output of the plate. We believe that both functions can be achieved in other ways.

QC - The QC function of this heat-aging step relies on heat stressing poor contacts (mainly aluminum to tin oxide, but also aluminum to a-Si) in order to make them worse and therefore easier to detect. Poor contacts also result in poor adhesion of the aluminum and can usually be detected in the "peel" test that is carried out after sputtering of the aluminum (applying, then rapidly pulling off a 2" strip of tape). In the past six months, we have experienced several runs with heat-age failures (a drop in FF of more than 5%), but in these cases the plates affected also failed the "peel" test (see M-1.2.2).

Another way of achieving heat-age type effects is to heat the plates in some other process step. Laminating is one that takes plates to 150^0C, but for a shorter period than the standard heat-age test. In addition to the shorter exposure time to high temperature, using the lamination cycle would only provide input on thermal stability

after the module has been almost complete. But since heat-age losses are rare, lamination would still provide the important QC function of identifying bad product. A fall-back position will be to do the heat-age test on a sampling basis and use a much smaller, faster responding oven.

Power Gain - It is likely that heat-aging produces no long-term power gain. We know from past experience that the gain resulting from heat-aging can be obtained at different temperatures. Figure 8 shows actual conditions previously used by EPV personnel for heat-aging a-Si plates. A fit of the temperatures to log (time) results in a surprisingly straight line. The temperatures and times initially chosen for these tests were based on QC considerations, but all of them also resulted in power gains of the plates.

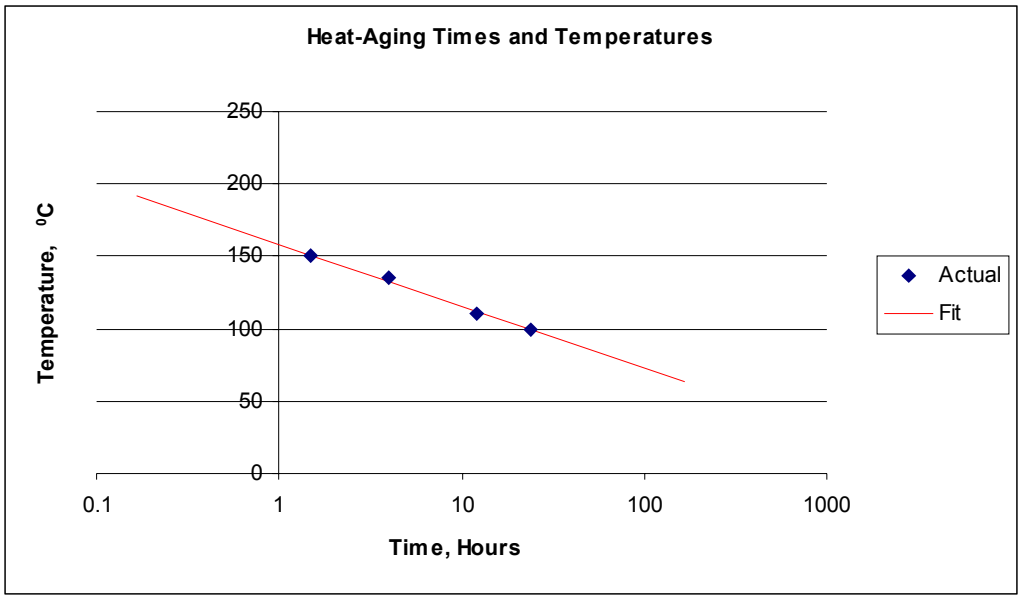

Figure 8: Relationship Between Temperature and Time of Previously Used Heat-Ages

If the extrapolations were to be valid, then at 55^0C (approximately corresponding to the module temperature that would be reached in full sunlight at 20^0C ambient), less than two weeks would be needed to realize the "same" effect as 1.5 hours at 150^0C. Whether this is actually the case is not known, but since it takes an a-Si module several months to stabilize it may well be sufficient to realize the heat-age gains. The net result would be that the modules would not have as large an initial Staebler Wronski degradation than if they had been heat-aged. Since our heat-age gain is typically 3-5%, the degradation would probably be reduced by that amount.

The encapsulation process was discussed as possibly serving the QC function of the heat-age test. It might also be effective in realizing the power gain. A test was carried out to investigate this possibility. Four plates from a run were not heat-aged, but instead passed through the lamination process several times. Their output changes were then compared to plates that had been heat-aged. The results are shown in the Table 11. Comparisons are made with plates that have comparable output prior to laminating.

Table 11: Using Lamination Cycle for Heat Aging Power Output Gain, %

Process step	Power Gain, %
Heat-aging (reference plate)	2.8
After first laminating cycle	2.6
After second cycle	0.0
After third cycle	0.1
After fourth cycle	-1.0

These results are only exploratory and do not include enough samples to make them reliable, but are sufficiently encouraging to warrant additional testing. In future tests, the plates that go through the lamination cycle will then be heat-aged to determine whether they have gained everything there is to gain. Another approach will be to monitor the detailed changes in electrical parameters of a plate that take place during the heat-aging step, by measuring dark IV parameters. These tests are in progress and use the laminator as the "oven". The laminator heats the plates rapidly and avoids the ill-defined (as to effect) heat up period of an hour or more that is needed in the heat-age oven.

Cost Saving - Labor cost savings from eliminating heat aging or combining it with the lamination process can be determined in the ideal case in which there are no "heat-age" losses.

The current heat-age process including transferring the plates to the oven, loading and unloading the rack takes approximately 1.5 minutes per plate. An additional 2 minutes is taken up by a measurement step. Eliminating both will result in a labor savings of 3.5 minutes or 4.4 %. No extra procedures are needed if the lamination process is used to obtain heat-age information, because the before and after IV tester measurements are also done in the process currently used. A small saving in electricity will also be realized.

B. Shuntbusting Process

Lasering of the aluminum back contact separates the individual cells, but leaves many cells with residual electrical shorts in the range of a few hundred to a few thousand ohms. Some of this shunting is the result of incomplete separation (see also M-1.2.2 above). Reverse biasing or shuntbusting the shorted cell at 4-5V, usually removes most of these shunt resistances. In our current process, shuntbusting is done at three locations (two ends and the middle) of each cell and for each photovoltaic (PV) plate.

We have determined that very similar results can be obtained by treating the entire PV plate or module at one time. This is done by discharging a small, 270-microfarad capacitor, charged to approximately 150 V, through the plate in the forward direction. This procedure also eliminates most shorts and typically gains an additional 1-2% of the measured power when applied to a finished module that had already been shuntbusted cell-by-cell. The procedure works well for tandem modules, but is not as effective when applied to single junction modules, because the voltage developed

across each cell is only about 2 V (with the capacitor charged to 150 V).

To evaluate this procedure, several tests were carried out in which the plates are first shuntbusted as full plates and then cell-by-cell. For three such tests, the average changes in electrical parameters resulting from the full-plate shuntbusting and subsequent cell-by-cell procedure are given in Table 12.

Table 12: Full Plate and Cell-by-Cell Shuntbusting

	Voc	**Isc**	**FF**	**P**
Change after full-plate shuntbusting (%)	2.1	-0.3	3.5	5.3
Change after additional cell-by-cell (%)	0.1	-0.1	1.3	1.2

The reverse order was also done, following the cell-by-cell shuntbusting of 23 plates by full plate shuntbusting. This second procedure resulted in a 2.5% additional gain in power output (other parameters were not recorded). Two to three percent is also the typical gain obtained when completed modules, which had been routinely cell-by-cell shuntbusted, were subjected to full plate shuntbusting procedure during their final IV test prior to packing.

An IV test, as currently performed, consists of a low light level Voc (LLLVoc) measurement, followed by the measurement of the IV curve. The effectiveness of the aluminum lasering can be judged by the improvement in the plate's electrical parameters that result from shuntbusting. Of these, the LLLVoc parameter is the most sensitive measure of shunting. Currently, the IV measurements are made both before and after the cell-by-cell shuntbusting.

Cost Savings - The process of carrying out the cell-by-cell shuntbusting takes approximately 2 minutes per plate. EPV's total labor content per module is approximately 81 minutes. In order to track the quality of the aluminum lasering we currently measure the IV of the plates both before and after shuntbusting, each measurement taking approximately 1.5 minutes. Full plate shuntbusting, as part of the IV testing measurements, is done automatically and requires no additional labor beyond that needed for the routine IV testing. The effects of the shuntbusting can be determined from the LLLVoc measurement that is performed prior to the IV measurement if it is also repeated after the full plate shuntbusting. The labor requirements of the new and the original process are summarized in Table 13.

Table 13: Processing Times With and Without Separate Shuntbusting

Process Step	**New Process**	**Original Process**
Plate IV Measurement	-	90 sec
Plate LLLVoc	1 sec	-
Full Plate Shuntbusting	1 sec	120 sec
Plate LLLVoc	1 sec	1 sec
Module IV Measurement	90 sec	90 min
Total (in minutes)	1.5 min	5.0 min

The 1.5 minutes for the IV measurement includes handling of the PV plate and periodic calibrations of the IV tester. By combining the shuntbusting with the IV measurements, a net labor savings of time is 3.5 minutes or 4.4 % is realized.

M-1.4.1 - Introduce Thinner and/or Lower Cost EVA onto the EPV Production Line

EPV has investigated two areas in which direct material cost reductions can be realized; less expensive EVA and a less expensive adhesive for the boot and bracket adhesion. Lamination problems that came up during this work are discussed below.

EVA - The cost of the EVA in the thickness range of interest, 12-18 mils, is nearly proportional to its thickness. Since we currently use an 18-mil product, the change to 12-mil thick EVA will result in cost saving of approximately 30%. No difficulties were expected in using the thinner material and none were encountered. About twenty modules have been made with the 12-mil material. No lamination problems were discovered with these modules either in the lamination process or with the finished modules.

Prior to making these modules, a problem of excessive bubble formation around the perimeter of the modules (using 18-mil EVA) needed to be solved. Later in the program during routine encapsulation, a serious delamination problem came up, apparently resulting from incompletely cured EVA. Both were corrected. In dealing with the delamination problem, a semi-qualitative test was developed for determining the degree to which the EVA had cured.

A. Excessive Bubbles

To be able to work around the bubble formation, numerous clamps were used to prevent these bubbles from forming. The problem appears to result from the edges of the glass being forced closer together than in the bulk of the module and results in EVA being forced out. When the lamination cycle is complete and pressure is released, the glass tends to return to being flat by the glass spreading apart at the edges, and air is sucked in between the glass sheets.

By preventing the glass from being squeezed together closer at the edges than elsewhere the problem can be avoided. Placing spacers around the perimeter of the laminates accomplishes this. The spacers reduce the force exerted by the bladder at the edges, and thereby prevent EVA from being squeezed out as the glass is pushed down. Avoiding the use of clamps also reduces the labor required for the lamination step by about one minute each. The 18-mil EVA was used for testing to define the best size and position of the spacers. The same solution worked for the thinner, 12-mil material where less EVA is available to be squeezed out.

B. Delamination

Delamination showed up at the corners of modules where it appeared that the EVA was not bonded to the plain glass. By cutting off a corner from a module that exhibited this problem, we discovered the EVA could be cleanly separated from both pieces of glass. Because the problem exists mostly on the corner and sometimes the edges, it appeared that it is due to non-uniform (and partially insufficient) heating during part of the lamination cycle. The EVA approaching its shelf life may also

contribute to the problem. Insufficient heating was confirmed when thermocouples were embedded inside a module and the temperature of the EVA measured during the entire lamination process, from preheat to cool down. Edges were approximately 10Cº cooler than the middle and corners about 20Cº cooler.

To obtain a quantitative measure of the extent of EVA cure, samples were prepared for gel content determination. These tests were carried out by STR (Specialized Technology Resources, Inc.) with whom we are cooperating on their own PVMaT contract (by supplying them with samples to laminate).

While preparing the EVA test samples, we also evaluated a test procedure for checking extent of cure of the EVA by a non-chemical means. The procedure is based on an STR "go/no-go" test and involves hanging a small weight (office clip) from a narrow strip of the EVA to be tested while it is exposed to 80-90^{0}C in ambient air. The EVA passes the test if, after 10 minutes, the strip has not elongated significantly (e.g. more than 10%). We have attempted to make the test more quantitative by precisely controlling test conditions, and by making continuous measurements during the test. EVA samples were made by placing an eight by eight inch sheet of EVA on top of a sheet of 1/32" thick Teflon. Another thin sheet of Teflon was then placed over the EVA and the sandwich preheated for the standard amount of time. It was then placed in the laminator and covered with a piece of glass and laminated using a range of press times between 70 seconds and 310 seconds.

We have applied the test to both 12-mil and 18-mil samples and have sent samples from the cured films to STR with mixed results.

Figure 9 shows the result of the stretch test for six samples and the Table 14 gives the gel content measured by STR. The graph shows why this is a go/no go test. The dividing line between the sample stretching quickly and hardly at all is a relatively small 10% range in cure times.

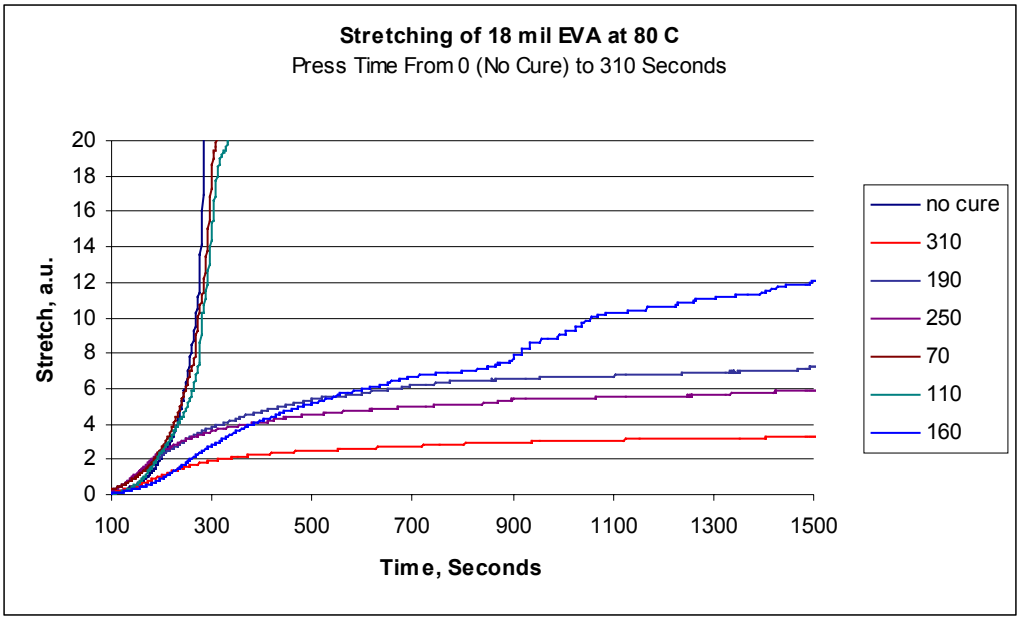

Figure 9: Effect of Lamination Press Time on EVA Cure Stretching at 80 C

Gel content determinations for some of these samples are given in Table 14 below. Both the gel content (nearly zero) and the stretch test suggest that the 12-mil EVA is not cured, yet modules made with the material appear to be well bonded and show no signs of insufficient cure – contrary to the delamination we discovered earlier with the 18-mil material. This discrepancy is being further investigated.

Table 14: Lamination Press Time and Gel-Content

Press Time, sec	Gel-Content, %
18 – 70	48
18 – 110	42
18 – 160	67
18- 190	77
18- 250	83
12 – 70	5

C. Adhesive

In addition to testing lower cost EVA, we have been testing a new adhesive for both the protection of the terminal connection and adhesion of the brackets. This material is a single–component, room–temperature-cure silicone compound. Its advantages include a lower material cost (approximately 1 cent per watt) and more importantly, the fact that a complex and expensive mixing station is not required. The absence of a mixing station avoids the possibility of using improper mixing ratios, a problem that we have experienced on several occasions.

Because mixing is not required for this new material and the equipment for dispensing it is relatively inexpensive, separate dispensers can be employed at both the terminal boot filling station and the bracket application station, making for a more streamlined operation.

The new adhesive is a one component neutral curing elastic adhesive/sealant that cures at room temperature when water is absorbed in the form of moisture in the air. The curing rate is a function of the amount of air moisture available, temperature, and the size of contact area to air moisture. A skin is formed in approximately 15–30 minutes. The bonding strength of the aluminum bracket to glass is primarily controlled by the cohesive strength of the material (bonding to itself) rather than the adhesive bond to the aluminum or glass surfaces.

D. Adhesive Thickness Tests

The maximum static tensile strength of aluminum bonded to glass was measured for various thicknesses of the new adhesive. The tensile strength was measured after the samples were left to cure for at least three weeks to ensure the adhesive was

completely cured. The pull tests recorded a value of 404 psi (pounds per square inch) for an adhesive thickness of 0.010 inches; 383 psi for a thickness of 0.020 inches and 360 psi for a thickness of 0.040 inches. Thus, the adhesive thickness is not a critical parameter, from the viewpoint of bracket bonding strength.

EPV's modules with the aluminum brackets bonded to its glass back surface using this adhesive were tested by UL for static mechanical loading. The modules were subjected to 10 days of humidity-freeze temperature cycling prior to actual testing. The aluminum brackets had a cross-sectional area of 6 inches in length by 0.75 inches in width (4.5 square inches), and the adhesive thickness was 0.010 inches. UL requires the module to withstand a positive and negative load test of 45 pounds per square foot with no visible signs of structural or mechanical damage. The test results were positive and the modules were judged eligible for using the UL mark. The force of 45 pounds per square foot means a total force on the EPV-40 module of 382 pounds. This is equivalent to a directed wind load of 100 mph (miles per hour) with a safety factor of 50 percent. The calculated tensile strength of the 6 inch long bracket has a total bond strength using this adhesive of approximately 1800 pounds (0.01 inch adhesive thickness), implying one bracket can withstand the entire force of 382 pounds, and the 6 inch long brackets can be reduced to, at least 3 inches in length, and still pass the UL test.

E. Cure Time

The tensile strength of aluminum bonded to glass was measured as a function of curing time over a period of several weeks. The surfaces of the one-inch by one-inch, 0.020 inch deep groove aluminum samples were wire brushed and all mating surfaces were cleaned using mineral spirits. The bonding surface of the aluminum samples, were pulled to obtain tensile strength data at fixed times after applying the adhesive. The experimental results are shown in Figure 10 as tensile strength versus curing time.

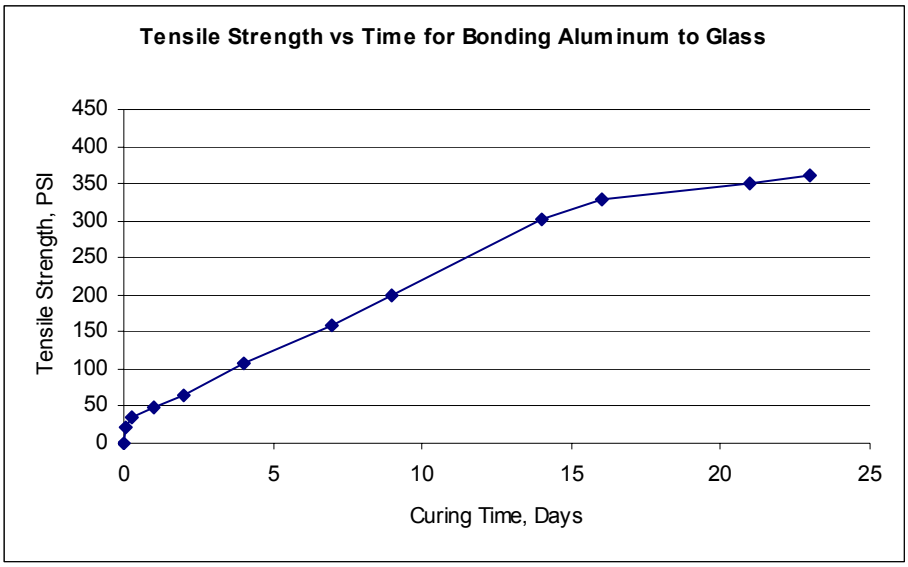

Figure 10: Tensile Strength of new Single Component Adhesive

The data show a rapid increase in tensile strength reaching 23 psi (an approximately 100 pound force for the six inch bracket) in three hours, and 50 psi in one day. The tensile strength then continues to increase steadily over time and reaches its maximum value of about 380-400 psi in several weeks. It should be noted that later tests using 0.010 inch thick adhesive show a more rapid curing time than for the 0.020 inch thick adhesive. The measured values are given in units of psi since the test samples were one square inch in area. However, one should note that the data represents the tensile strength of only that fraction of the sample area that contains the cured material. In reality, the experimental data, in the early stages of the curing cycle, is a measure of the percentage (relative to the maximum tensile strength) of the sample area that contains the cured material. It was observed that the adhesive material "wetted" both aluminum and glass surfaces immediately. This is expected since the adhesive has a built in primer.

The tensile strength of the entire aluminum bracket was also tested as a function of curing time for the standard 6-inch long bracket, with a surface area of 4.5 square inches. The experimental data of pull strength versus curing time is shown in the Figure 11. The experimental data was limited to 300 pounds of force because of the limit of the testing apparatus. Two sets of data are shown for the 6-inch long standard aluminum bracket which were wire brushed and all mating surfaces cleaned using mineral spirits. One set is for the brackets with a 0.010 inch deep groove, and the other set of data corresponds to brackets with a 0.020 inch deep groove for the adhesive.

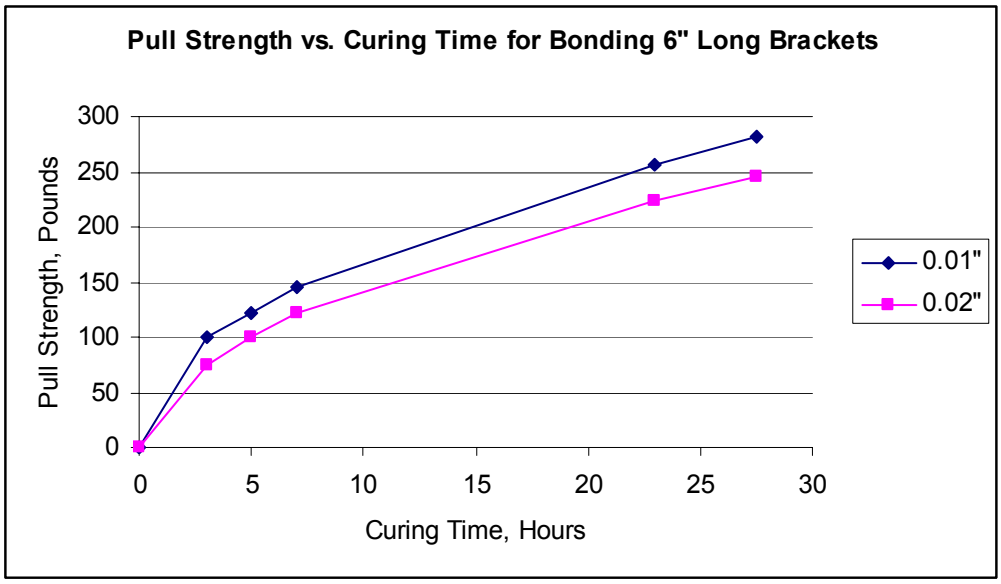

Figure 11: Pull Strength of New Single Component Adhesive

As expected, the data clearly demonstrates the tensile strength of the standard 6-inch long bracket is higher when using the 0.010 inch thick adhesive than when using the thicker adhesive of 0.020 inches. Even though the adhesive material takes several weeks to completely cure, the 6-inch standard bracket has a pull strength of 100 pounds in three hours and 260 pounds in one day. The good bonding strength

achieved in three hours, allows movement of the module with little risk of bracket movement. This makes the use of this adhesive compatible with the process currently being used at EPV to attach the standard 6-inch long brackets, since in both cases, the brackets are held in place with tape until sufficiently cured.

The conclusion of these experiments is that the one-component, low-cost adhesive can be employed to attach the brackets without changing the current production process. In addition, the data suggests that the current production process of attaching the wire "boot" and the four (4) brackets could be now done at two separate stations thereby eliminating the need for two separate dispensing guns attached to the mixer / dispenser machine currently used.

M-1.4.2 – Upgrade RF Matching Network on One Section from Manual to Automatic

To aid in the building of a matching network specifically designed for our deposition system, tuning parameters were determined for the RF discharges employed in our process. The effect of high reflected power was also investigated. The matching network used for the tests consists of a typical "L" topology with two variable capacitors, the input capacitor to tune to the RF generator and the output capacitor for tuning the plasma load.

In the first test, the reflected power was measured while changing the values of the capacitors one at a time, holding the other capacitor fixed. As the graph below shows, the input capacitor has relatively little effect on reflected power. The capacitance values are the deviations from their original tuned value.

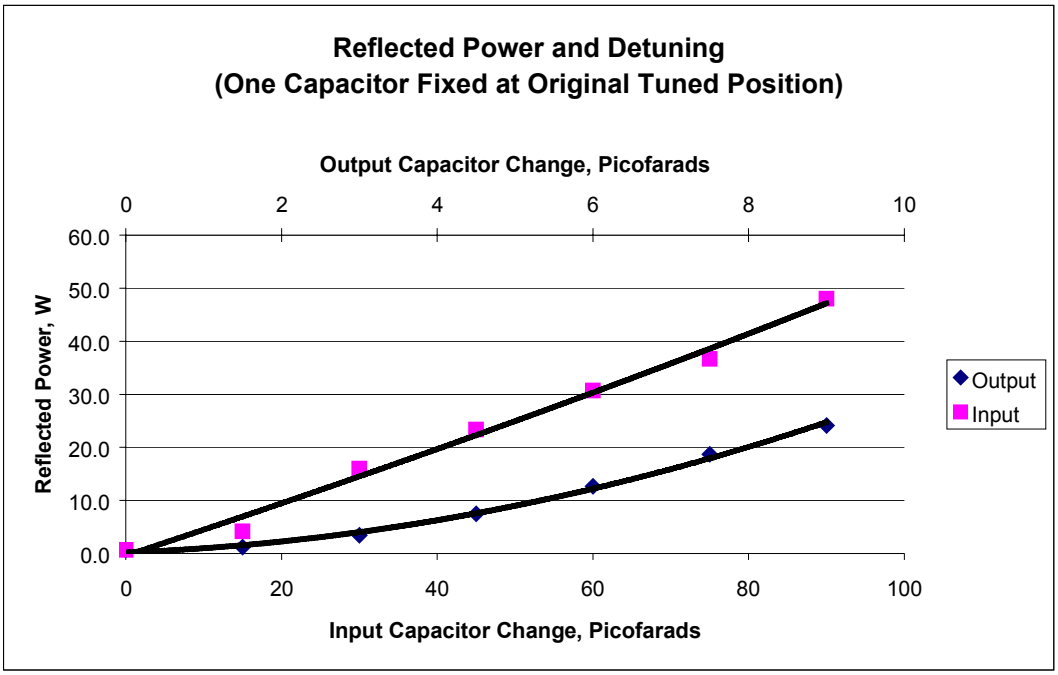

Figure 12: Effect on Reflected Power of Detuning Capacitors in RF Matching Network

The effect of pressure changes was also investigated and found to be small.

Restarting the discharge ten times and tuning for minimum reflected power checked repeatability. As seen in the Figure 13, the output capacitor is within a range of approximately 5 picofarads for the ten tests which, from the graph above, corresponds to approximately 30 W reflected power.

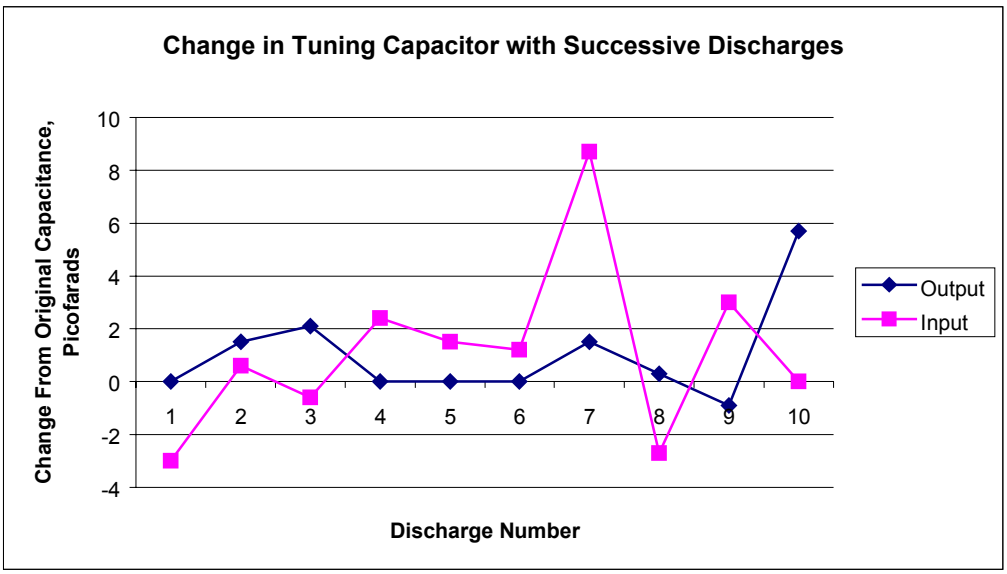

Figure 13: Repeatability of Capacitor Setting in RF Matching Network

To determine if a reflected power level of 30 W has any effect on the quality of the plates, a run was made in which two sections were deliberately detuned to achieve a reflected power of 75 W, or approximately 30% of the input power to the matching network. In this test, the RF current delivered to the discharge was held constant. Averaged electrical parameters of the plates made with a 75 W reflected power, and the plates made with essentially zero reflected power are summarized in the Table 15.

Table 15: Electrical Parameters With and Without High RF Reflected Power Averaged Electrical Parameters

Reflected Power (W)	Voc (V)	Isc (A)	FF	P (W)
75	62.9	1.24	63.6	49.7
0	62.7	1.22	63.1	48.4

No significant difference between the plates was observed. As a result, a very simple automated matching network is contemplated that simply pre-selects the capacitor setting that brings it to the approximated point needed for low reflected power. By tolerating a reasonable amount of reflected power, a precise feedback-controlled tuning device is not required.

Such a matching network was built and is currently being tested.

M-1.4.3 - Complete Study of Process Steps and Establish Most Promising Approaches for Automation

We have reviewed our current manufacturing process and estimated the cost and gains resulting from automating various steps.

From this analysis two process steps were selected as candidates for automation in Phase II. The selection was based on two major criteria, that is 1) reducing the direct labor component of that particular step, thereby reducing product cost or 2) upgrading or replacing the equipment in that process step to improve the equipments reliability, performance, and throughput; and/or increase the quality of the equipment's output. The two process steps tentatively identified are 1) automating the seamer and the seamer to washer transfer, and 2) the sputtering system unload and stack.

A. Seamer

Here the second criteria, improving equipment performance and quality of output is the primary desired outcome. The currently used seaming operation involves the use of a Prestik 2 belt wet seamer using 2 - 4" X 106" 80 grit sanding belts and a 36" X 78" roller table. The belts are diagonally opposed to each other to lay a seam or slight bevel on all 4 edges of the glass substrate. To seam a piece of glass the operator must rotate the glass substrate on the roller table while maintaining contact with the 2 belts. We have found this process to have an inherent repeatability problem both from the operator 'processing' side and from an equipment side as the sanding belts wear down. As edge defects are a primary cause of plate and module breakage as the substrates are stressed, the importance of producing a uniform, seamed edge cannot be minimized. The intention is to replace the current equipment with a heavy duty single or multi-spindle automatic glass edger (i.e. like the Somaca VE-1A). This, or a similar machine, has the capacity to produce various uniform and consistent edges like a pencil edge and/or a flat, seamed edge that is not operator or sanding belt dependent. There is also the possibility of increasing throughput and of reducing labor costs by adding an edger to the washer transfer mechanism.

B. Sputtering Unloader

Reducing labor costs, is the primary motivation for selecting this step. Automating this step would also resolve an employee health and safety issue. The current setup involves the use of EPV's proprietary automated inline sputtering system. While the inline system itself has the capacity to run in a fully automated mode (i.e. move the substrate through the various load locks and sputtering chambers), to meet the required throughput an operator must still be available to unload the substrate at the proper time. It is the desire here to replace that part of the operator's time completely with a fully automated system that will 1) open the exit chamber door, 2) transfer the glass to a buffer type storage area to await aluminum scribing, and then 3) close the exit chamber door. This system will also eliminate a potential health and safety issue as the current unload procedure requires the operator to remove the substrate from the exit chamber at an exit chamber height of nearly 60 inches.

M-1.4.3 - Complete the Phase I Portion of the Effort Under Task 1.

Phase I portion Task 1 was completed.

3.2 TASK 2: STABILIZATION OF PV MODULE POWER OUTPUT – I

The objective of this task was to increase the stabilized power output of EPV's a-Si modules through improvements in device efficiency and optimization of module design to increase the active area of the modules. This task resulted in an approximately 10% increase in stabilized module power output which, together with the reduction in manufacturing cost resulting from Task I, resulted in more than a 20% reduction in the module cost per watt from the Energy Photovoltaics production line.

M-1.2.3 - Increasing the Active Area of the EPV a-Si Module Product by 5%

There were three areas in which increases in active area were attained, narrower aluminum foil, narrower scribes and a more optimized layout of the scribe patterns.

A. Narrower Aluminum Foil

A small gain was obtained from changing the foil width from 6.35 mm to 4.76 mm. This change resulted in an increase in active area of twice (6.35-4.76)/60 or 0.5%.

B. New Layout

A somewhat larger gain was achieved with an optimized, more symmetrical cell layout. Prior to the change, the distance from the module top edge (as placed in the deposition system) to the first cell was approximately 16.9 mm. This distance at the bottom was 27.3 mm. In addition, the foil bonded to the top cell would often overlap (sometimes only partially) the next cell, thereby causing the loss of the most of the output of a cell on one end. With the new laser pattern, narrow end cells, only 0.01" wider than the aluminum foil, were placed such that the foil butted up against the sandblast area (the alignment and precision of the foil bonder was also improved to accomplish this). The remaining area was then divided into 38 cells. The layout placed the first active cell only 17.2 mm from the edge, both at the top and bottom. Excluding the gain from the narrower foil, an additional 1.5% gain resulted from this more efficient layout.

C. Narrower Scribe Width

The initial attempt to reduce the scribe width focused on improving the tracking of the two xy tables used for lasering (an IR laser for tin oxide and a green laser for silicon and aluminum). This was only marginally successful. In some cases improvements of approximately 2% were obtained but they were not very consistent.

To routinely achieve a significantly narrower scribe width, either active tracking has to be employed or only one xy table used for all three scribes. The latter was used for several runs on a trial basis and has now been adopted for all lasering. The improved alignment achievable with this approach has resulted in a reduction of the total scribe separation from approximately 0.92 mm to 0.23 mm. The narrower scribe width adds about 4.1% to the active area making the total gain 6.5%. When an additional cell is lost because of foil overlap, the loss adds another 2.6% to the gain obtained from avoiding this loss, although the entire output of that shorted cell is not typically lost. From a small sample of 14 modules, 11 had foil overlap of the first cell. If we

assume that half the output of the shorted cell is lost, an average of 1.3% additional loss occurs, to bring the total gain achieved in the new layout to approximately 8%.

The one downside of using the green laser for scribing the tin oxide is that more power or a slower table speed are required. To use a single xy table in manufacturing, either both an IR and a green laser would have to be mounted on one xy table, or more likely, a more powerful green laser has to be used for all three operations.

For single junction modules, the gain in active area is even more dramatic because of the narrower cells. In this case the corresponding gains for the three changes are 0.5%, 1.3% (because a smaller cell is gained) and 9.4% for a total of 11.2%.

Other implications of using one xy table for all scribes in a manufacturing line is the change in equipment layout that is needed to accommodate the plate transport from deposition and sputtering back to the same xy table used for the tin oxide lasering.

M-1.3.2 Complete Analysis of Higher Quality Tin Oxide Availability and Effect on Product Performance

Module performance has been increased and costs have been lowered through the optimization of the transparent conductive oxide (TCO) front contact. This work was accomplished through a cooperative effort with our tin oxide suppliers.

A total of nine variations of TCO were obtained from our suppliers and tested. The analysis proceeded in two stages starting with single junction modules and then progressing to tandem modules. The data for the two sets of tests are shown in Tables 16 and 17. The "S" prefix denotes a standard product and an "E" prefix denotes an experimental TCO. The two manufacturers used in this optimization are identified as manufacturer 1 (M1) and manufacturer 2 (M2). The standard types of TCO used in our facility are S1-M1 and S1-M2.

Table 16: Single junction test results of seven types of TCO

TCO Type	Voc	Isc	FF	Power
S1-M1	**1.000**	**1.000**	**1.000**	**1.000**
E1-M1	1.001	1.039	0.989	1.028
E2-M1	0.992	1.024	0.993	1.008
E3-M1	0.996	1.031	0.981	1.007
E4-M1	1.000	1.044	0.998	1.021
S1-M2	**1.006**	**1.054**	**0.978**	**1.036**
E1-M2	1.009	1.000	0.982	0.990

Table 17: Tandem junction test results of nine types of TCO

TCO Type	Voc	Isc	FF	Power
S1-M1	**1.000**	**1.000**	**1.000**	**1.000**
S2-M1	0.997	1.010	0.980	0.986
E1-M1	1.005	1.043	1.000	1.048
E2-M1	1.006	1.039	0.982	1.027
E3-M1	1.001	1.035	0.994	1.029
E4-M1	1.003	1.039	0.988	1.029
S1-M2	1.005	1.053	0.976	1.033
E1-M2	1.010	1.044	0.970	1.023
E2-M2	**1.015**	**1.049**	**0.985**	**1.049**

In the single junction study, we observed that the standard product S1-M2 TCO outperformed all other types of TCO. However, several manufacturers of PV products including EPV noticed that this TCO was sometimes prone to delamination and therefore was not suitable for use in production [2]. By cooperatively working with the supplier, alternatives were developed that did not have this problem. The first experimental TCO from this supplier (E1-M2) was shown not to delaminate, but it did not perform as well as other products in our single junction tests. Meanwhile the other supplier developed four variations of their TCO, two of which looked promising (E1-M1 and E4-M1).

In the second stage of our testing, tandem modules were tested on these same TCO varieties with the addition of a new improved version from manufacturer 2 (E2-M2), and a second standard product from manufacturer 1 (S2-M1). The results on our standard tandem modules were very encouraging. Two types of TCO emerged as being superior to the previous standard products. The new type E2-M2 was 4.9% better than the reference TCO, followed closely by E1-M1, which was 4.8% better. In addition, all of the experimental TCO types were shown not to delaminate during testing.

Manufacturer 2 was so convinced of the improvements made in their latest version of this TCO that they made the E2-M2 TCO their standard product. Subsequent modules made on this TCO have demonstrated their robustness in preliminary outdoor exposure tests and so this was adopted as an EPV pilot line standard TCO. Concurrent with the TCO optimization, EPV negotiated a 23% cost reduction for this TCO.

M-1.4.5 – Demonstrate 10% Increase in the EPV a-Si Module Stabilized Power Output

In addition to the higher stabilized output a great deal of effort under this task went into measurements, especially outdoor measurements. This effort supported other tasks in addition to this one (e.g. comparing single junction and tandem modules, reduction in cycle time etc.) Preliminary work on a ZnO/Al back reflector was also begun in preparation of making full size modules in Phase II.

A. Increased Output

Achieving an increase in stabilized power output was pursued on several different fronts. The first and most significant gain was achieved by optimizing the layout of the module including narrowing the separation of scribes between cells. This combination resulted in a gain of approximately 8% in active area and output (see M-1.2.3 above).

Active area is easiest to quantify, while other gains are not as easily demonstrated because of variations between modules and runs even when made under the same conditions. Some increase in output can, however, be attributed to greater attention to paid to reproducibility and deposition procedures, especially cleaning of the box carrier between runs. The improved cleaning was intended to minimize the amount of particulates in the chamber and thus reduce the extent of shunting between cells. Some of the inserts in the box carrier are placed there to prevent discharges on bare metal. After a few runs, these became heavily coated and then often flaked badly from the accumulated silicon. A rigorous schedule of replacing these inserts together with a more thorough cleaning of the box carrier between runs has reduced the amount of shunting considerably. A reduction in RF power is likely to also have contributed to the reduction in powder generated during the discharge. Gains from this source are not as easily quantifiable as increases in active area, but together with tighter control of process conditions, this source is believed to have achieved the additional two to three percent gain that is required to reach the ten percent goal. Recipe changes were also evaluated but results are still inconclusive.

Figure 14 below shows the FF obtained for a series of consecutive runs, some from prior to the instituting the improved cleaning procedures and some after these were started. Note that some runs were excluded, primarily because they did not go through the standard process.

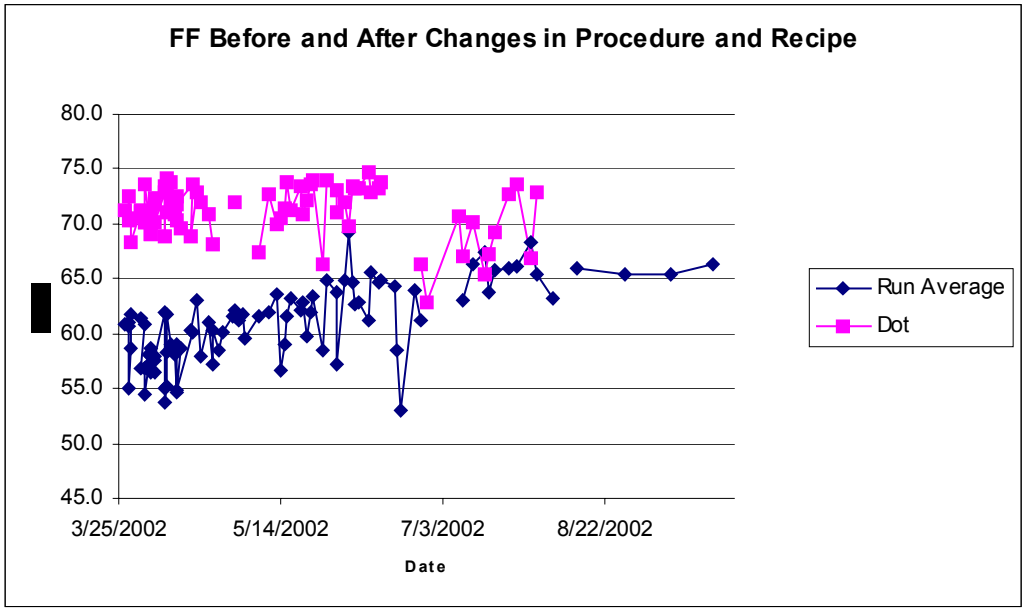

Figure 14: Fill Factors Before and After Improved Processing

The upturn in FF starting just prior to this program's officially beginning (in July) can clearly be seen. The fact that dot FF did not change support the assumption that the gains in module FF are the result of processing changes.

B. Measurements

To determine performance, modules must be subjected to extended light-soaking. An expanded outdoor light-soaking program has been undertaken to provide the necessary information. In most of our light-soaking studies, we bring modules inside to measure on our flash IV tester. Since we expanded the light-soak program, some modules were placed in a relatively inaccessible roof location requiring more measurements to be made outdoors. This requires finding a means of obtaining IV data outdoors and calibrating a reference standard to measure light intensity levels. Outdoor measurements are made with either a small microprocessor based portable tester (based on an Onset Computer Corp. Tattletale Model 5) or a dedicated data acquisition system (using a Campbell Scientific CR10X data logger).

To calibrate outside measurements, a series of comparisons were made over a period of approximately a month in which eleven modules were repeatedly measured both indoors and outdoors. The purpose of these measurements was to obtain an estimate of the reliability of outdoor data and to calibrate the reference cell used outdoors. Light-soaked single junction and tandem modules and as-made (not light-soaked) single junction and tandem modules are included in the comparison. The first comparison indicated that the photodiode reference value resulted in modules having an output approximately 4% too high – this was corrected. Temperatures, both of the modules and the reference cell were also investigated.

Reference cell - When measuring modules outdoors, we measure IV parameters, module temperature (on the front surface), and photodiode output; however, we do not measure the photodiode temperature. Typically the output of a photodiode is either measured as a current or as a voltage (with a load resistor). In either case, the operating point of the diode will be low enough to effectively measure the short circuit current. This current will be temperature dependent. Because temperature coefficients for current and voltage have opposite signs, using a higher operating point (than typically used) should result in a lower, possibly even zero, temperature coefficient. Tests were completed to determine the extent that the temperature sensitivity could be reduced. Figure 15 below shows the output current of a 1-cm^2 area UDT Sensors, Inc. silicon detector at constant illumination as a function of temperature at operating points between 130 and 324 mV.

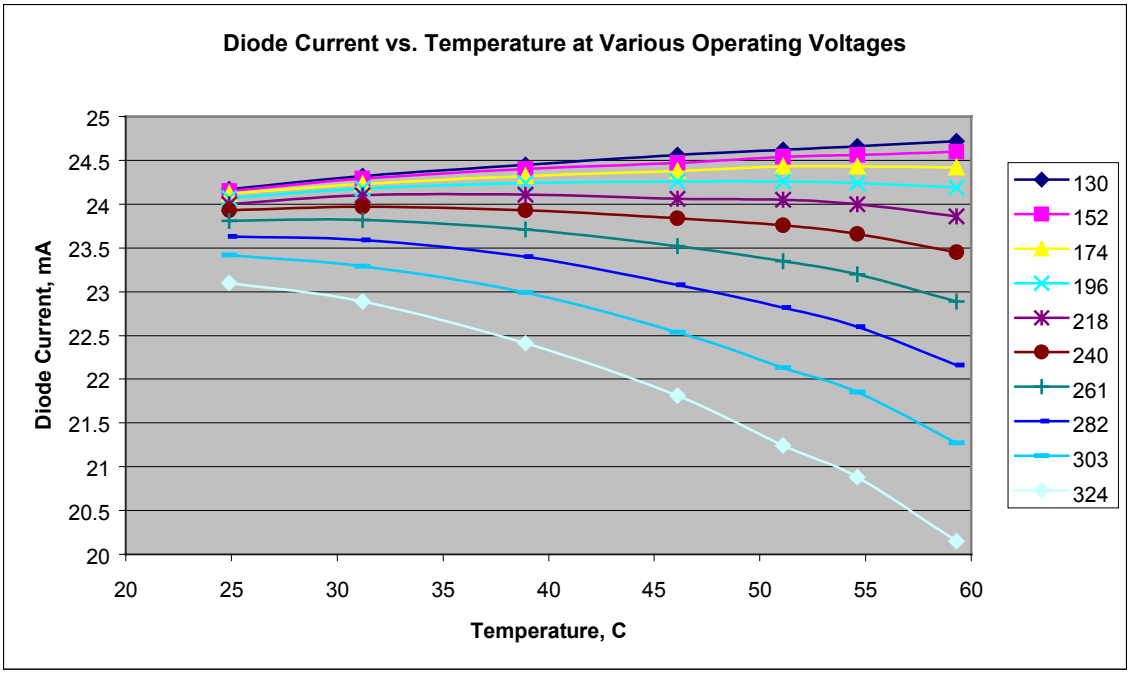

Figure 15: Effect of Temperature on Diode Current at Different Operating Points

Even though the changes are not linear, there is a significant, nearly straight region at the lower voltages, and at 223 mV (interpolated from the above data), the output is constant to within 0.35% over the 20 to 50° C temperature range. At short circuit, the output variation over this temperature range would be a factor of approximately five times higher (corresponding to a temperature coefficient of 0.11%/°C). Testing under somewhat different conditions (using a constant load on the diode to achieve an operating point, instead of fixing it directly) showed that the "zero" temperature coefficient point to vary slightly with intensity. Whether this is the case with a well-defined operating point remains to be seen. To maintain the diode at approximately 223 mV an active circuit was built. To avoid having to use a battery, the small circuit was mounted on and powered directly by a small 3" by 4" a-Si micro module. The small module had a hole near one end through which the diode protruded so as to make it approximately flush with the face of the small module. The output of the micro module was enough to operate the device down to approximately 5% of one sun intensity. It was found that in most cases the difference between the output of this detector and the reference cell previously used was small, typically 1 to 2%.

Even with no uncertainty in the reference cell, there is some uncertainty in the module temperature. We measure the module temperature on the front or back surface, but the film temperature is not known. This is not necessarily a problem as long as the temperature measured is meaningful and stable. Unless modules are being light-soaked, outdoor exposure time is usually held to a minimum, and modules do not necessarily have time to equilibrate in temperature. This causes the temperature of the module surface and the inside thin films to not be precisely related. The magnitude of the effect on measurements was determined experimentally. Figure 16 shows Voc values taken 0.4 seconds apart for 400 seconds. Attempting to fit the

voltages to a single exponential decay resulted in poor agreement but two exponentials described the decay well as shown on the graph.

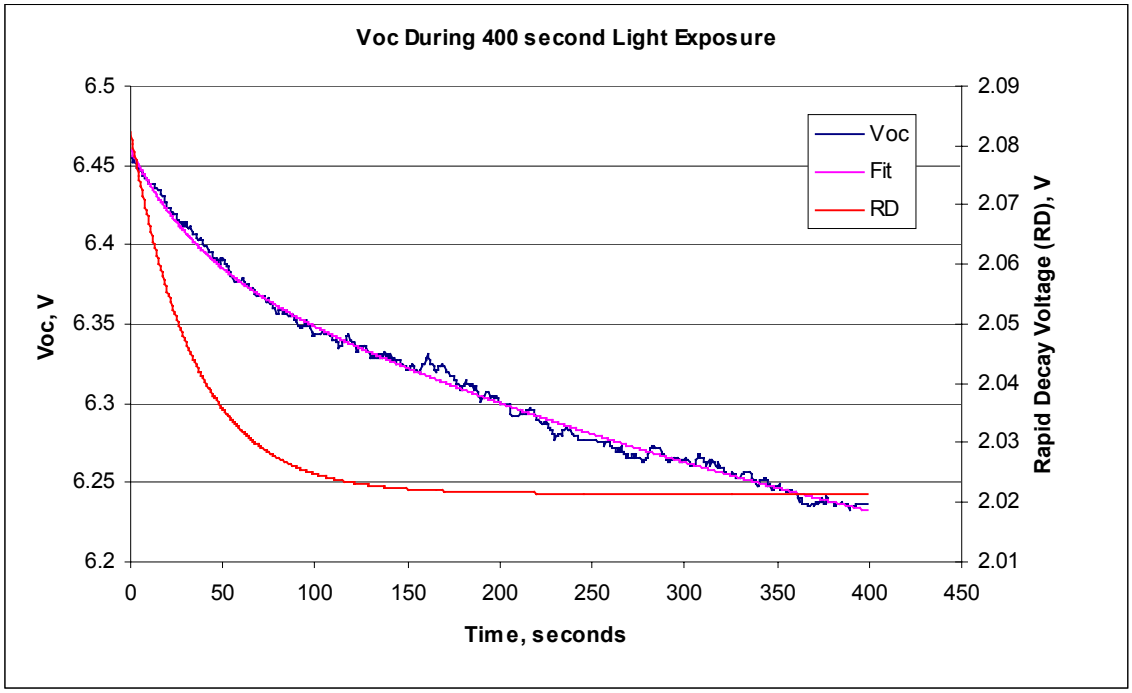

Figure 16: Change in Voc as Function of Time Exposed to Sun

The two exponentials have time constants of 34 seconds and 530 seconds. The rapid decay (shown in the graph as RD) corresponds to a voltage drop of approximately 1%, implying an approximate 3^0C temperature rise in 100 seconds. This temperature rise can reasonably be assigned to the initial temperature rise of the thin film. The slower decay amounts to approximately 5%, or 16^0C and is very likely due to the slower heating of the module glass. The rapid decay time-constant is of the order of the variation in the time required to position the module outside, make electrical connection, etc., and could therefore account for nearly 1% in Voc variations. To minimize errors resulting from these effects, an effort is made to keep the outdoor exposure the same for all modules measured.

C. ZnO/Al Back Reflector

In an effort to improve module efficiency, we have investigated the benefit of using a composite zinc oxide–aluminum (ZnO/Al) back contact. The standard back contact has been a simple sputtered aluminum back contact, and we have found that it does a good job of reliably collecting current from the a-Si at a reasonably low cost. However, it is well known that by inserting a transparent conductive oxide between the aluminum and the a-Si, the reflectivity of the back contact can be significantly improved [3].

.

1. Preliminary Small Area Studies - We began our investigation by using small test samples of a-Si cut from full sized plates produced in our pilot line. A single full sized plate was cut up into several small samples, approximately 5 cm x 10 cm,

and each of these was processed with either our standard back contact (Al only) or a sputtered ZnO/Al back contact. For our initial tests, we decided to use single junction a-Si to simplify the experiment. Small area devices were formed on these samples using an etching procedure and the QE currents were measured. A typical result is shown in Figure 17 below.

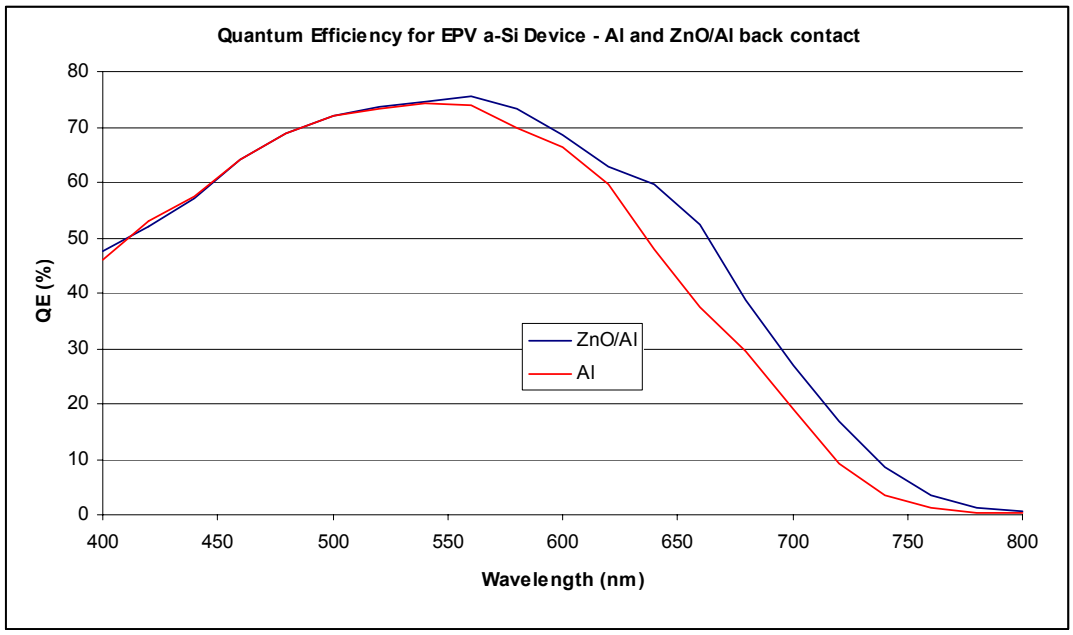

Figure 17: Quantum Efficiency Curves for EPV Single Junction a-Si With and Without ZnO Back Reflector

These initial tests show that we can significantly improve the long wavelength response of our a-Si by using a ZnO/Al back contact. It can be seen from the QE curves in Figure 17 that the Jsc for the ZnO/Al sample is 8.7% higher than the Jsc for the sample with the Al back contact. This improvement came from an increased long wavelength response, mainly between 550 and 750 nm. The ZnO clearly improved the reflectivity of the back contact resulting in greater absorption of light in the active semiconducting layers. This initial result was encouraging and further optimization was pursued to develop a process suitable for large-area modules.

In an effort to characterize the sensitivity of the current gain with respect to variations in ZnO thickness, a second series of experiments was conducted. In this series, the ZnO thickness was varied from 0 to 1600 Å and the Isc was measured for each small area cell. Once again, the same single junction silicon was used from the EPV pilot line to simplify the characterization. The results are plotted in Figure 18 below, along with a best-fit polynomial curve.

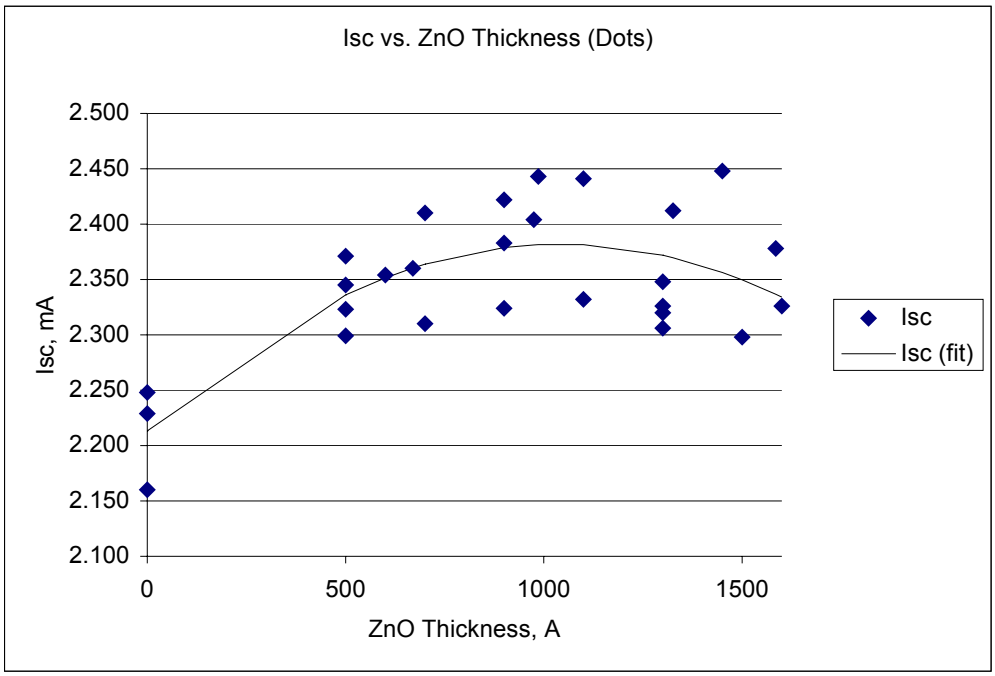

Figure 18: Small area cell Isc vs. ZnO thickness on EPV single junction a-Si

As also observed in the Figure 17, the data in Figure 18 clearly show that the presence of ZnO has a significant effect in increasing the cell Isc. The control samples with no ZnO clearly have the lowest Isc and it appears that initially the Isc increases with increasing ZnO thickness. Near approximately 1000 Å (±~100-200 Å), the increase seems to level off with increasing thickness, possibly saturating. Beyond ~1200 Å, the data seem to show a possible decrease of Isc with increasing ZnO thickness, however, the scatter in the data does not allow us to determine with any certainty whether the Isc drop observed in this experiment is statistically significant.

While it is clear that there is significant variation in the data, and thus the precise placement of the curve is subject to some uncertainty, it can be seen from the general shape of the curve that the Isc is not very sensitive to variations in the ZnO thickness. The peak centered around ~ 1000Å is very broad, which indicates that large variations on the order of ±20% have very little effect. This is an encouraging result that will help ensure high process yields when the ZnO process is introduced into the manufacturing environment.

The overall improvement in Isc is also very encouraging. The best sample measured in this experiment had ~ 1000 Å of ZnO and had an Isc that was 10.4% better than the average control group Isc. If we use the best fit curve to estimate the Isc of a typical sample with a 1000 Å ZnO back reflector sample, we find that the Isc is expected to be 7.7% better than the controls, a very good result that is in line with our previous experiments.

2. Initial Evaluation of Interconnect - Building upon the successes of the small area device work on single junction a-Si, we began developing processes on small

series-connected plates. The first mini-module plates that we tested were ~5 cm x 10 cm devices that were deposited in the same ZnO system used for the previous tests. We divided the initial experiment into three groups: 1.) control plates with no ZnO, 2.) ZnO back reflector plates with ZnO filling the interconnect scribe, and 3.) ZnO back reflector plates with Al filling the interconnect scribe. Due to a shunting problem unrelated to the back reflector, the module data was not useful; however, we were able to test the integrity of the interconnect under thermal cycling.

To test the interconnect, one sample from each of the three groups was thermally cycled between -10°C and 30°C; each cycle included at least 24 hours at –10°C. At regular intervals during the cycling, the interconnect resistance was measured across a single segment on each sample to determine if the interconnect was being degraded. We paid particular attention to the sample that contained ZnO in the interconnect scribe to determine if the thermal cycling would open that connection and consequently result in a high resistive losses. Over the course of 12 thermal cycles, the interconnect resistance was unchanged for each of the samples, within the measurement error. Based on this result, it appears that interconnects filled with ZnO are equivalent to interconnects filled with Al on ZnO back reflector modules when subjected to moderate thermal cycling.

3. Module Development - To develop a process suitable for large-area modules, we began using a pulsed DC sputtering system capable of depositing ZnO on substrates that are 48.25 cm x 91.5 cm (19” x 36”). Our initial experiments using this system were performed using single junction a-Si from our pilot line. Although several modules once again had some shunting problems, we were able to demonstrate the scalability of the process and produce a working module. The performance of the best module from this set of experiments is shown below.

Table 18: IV Parameters of Plate with ZnO/Al Back Contact

Plate #	263-21
Size	19”x36”
a-Si	Thin single junction
Back Reflector	500 Å ZnO:Al/Al
Voc	44.7 V
Isc	903 mA
FF	64.5%
Power	24.31 W

We used modules in this same series of experiments to optimize the i-layer thickness for use in a ZnO/Al back reflector module. Several modules were made with a range of i-layer deposition times (i-layer deposition time is proportional to thickness) and small area cells were tested. Theses same cells were subjected to a

47 sun accelerated light soak (ALS) and retested. The results of this experiment are summarized in Figure 19 showing i-layer deposition time versus small area (dot) Isc before and after accelerated light soak (ALS).

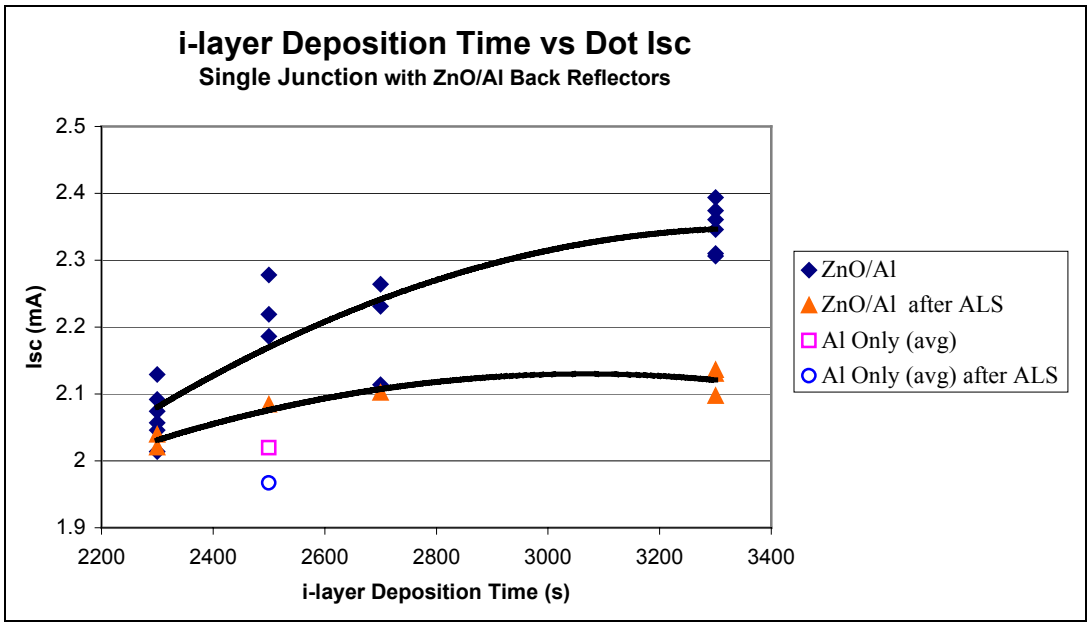

Figure 19: i-Layer Deposition Time Versus Small Area Cell Isc Before and After Accelerated Light Soak

The first interesting item to note is the difference between the before and after ALS curves. The top curve shows that the Isc of the cells before light soak increases with increasing i-layer thickness (time) and appears to have a maximum somewhere beyond 3300 seconds. However, the lower curve shows a much more gradual rise and the i-layer time for the maximum Isc is much lower, perhaps between 2700 and 3300 seconds. Although this is only a preliminary experiment, and more work needs to be completed to optimize the Voc and FF, it highlights the importance of optimizing the process for maximum stabilized performance, since the maximum Isc point clearly shifted after ALS. Based on this result (which is not unexpected), we will consider reducing the thickness of our single junction i-layer in future experiments in order to increase throughput and optimize performance.

The second item to note on the graph is that the net gain in Isc before light soak is 10.9%; this can be observed from the data at 2500 seconds. This is within the typical range for a cell with a ZnO/Al back reflector. However, it is interesting to note that the net gain from the ZnO is reduced after light soaking to 5.9%. This is due to a larger average percent degradation for the samples that have the ZnO/Al back reflector. If this trend holds true in further tests, we will need to revise our estimates for the expected current gain due to the improved ZnO/Al back reflector. This will be an important area for future study, particularly if this trend holds true for modules put into outdoor arrays. However, we expect that the outdoor results will have lower light soak losses than is indicated in this

experiment and the net gain in current will be higher than 5.9% after light soaking outdoors. The ALS tests tend to overestimate the losses caused by light soaking because they do not include the annealing effects present in modules light soaked outdoors.

4. Elimination of Shunting Problem - To successfully fabricate a high quality ZnO back reflector, we needed to eliminate the excessive shunting that we observed in previous runs. To this end, we carefully monitored the deposition, laser scribing, and handling processes to ensure that each plate was processed with a minimum of damage to the films prior to testing. We also took steps to ensure that the ZnO did not create leakage paths at the ends of each segment. In doing this, we developed an improved process that clearly reduced the incidence of shunting in modules with a ZnO/Al back reflector.

   In order to minimize the number of variables in our comparisons between plates with and without ZnO, we cut each test plate into three sub-modules immediately after a-Si deposition. Each sub-module was approximately 33-38 cm (~13-15 inches) wide by 63.5 cm (25 inches) long. We processed one section of the module as a standard module and processed the remaining sections with a ZnO/Al back reflector. Since the same a-Si was used on plates with the different back reflectors, we were able to accurately measure the effect of the ZnO.

   The results of this optimization were very successful. The ZnO process worked as expected and the modules showed significant improvement. The Table 19 below contains the results for the best module produced. The first two entries show the performance of the individual sub-modules, one with the standard Al back reflector and the other with ZnO/Al. Since the two sub-modules have different active areas (due to the difference in glass size) and thus the current and power cannot be compared directly, the data was normalized and scaled up to show the performance of an equivalent full sized plate, assuming that the Isc scaled linearly with area and the Voc and FF were constant. These scaled results are shown at the bottom of the same table. The projected power for the scaled-up ZnO/Al plate is an impressive 59.1 watts compared to 54.15 watts for the scaled standard plate, which is also a good result. This is a 9.1% gain in power. As expected, this gain is almost completely due to the increase in Isc, which is higher by 8.5%. The FF and Voc are essentially the same with or without ZnO, within measurement error, which indicates that the ZnO did not cause any shunting or series resistance problems as had been observed in earlier experiments.

Table 19: Comparison of IV Parameters of Plates With and Without ZnO/Al Back Contact

Description (plate # 265-22)	**Voc (V)**	**Isc (A)**	**FF (%)**	**Power (W)**
Std Al – sub-module as measured	63.42	0.335	68.51	14.41
ZnO/Al – sub-module as measured	63.74	0.391	68.56	17.04
Std Al – scaled to full sized module	63.42	1.246	68.51	54.15
ZnO/Al – scaled to full sized module	63.74	1.352	68.56	59.10

Overall, the results were very encouraging and are significantly higher than any typical modules made to date. We intend to further optimize the process on both single junction and then transfer the process to tandem modules. We will perform light soak studies and test modules outdoors to maximize module power and maintain high reliability.

M-1.4.6 - Demonstrate 20% Decrease in $/Watt for a-Si Modules from the EPV Production Line

Significant cost reductions were realized in both labor and material costs. The contributors to the reductions are: higher module output (with no increase in cost), elimination of shuntbusting as a separate operation, elimination of masking during sandblasting, reduction of deposition cycle time, and lower cost EVA. Details of the reduction obtained in these areas are covered in their respective sections of this report. In summary the cost reductions from these contributions are the following:

Table 20: Cost Reduction Achieved During Phase I

Higher output	10%
Eliminate shuntbusting	4.4%
Eliminate masking	9%
Cycle time reduction	1.5%
Lower cost EVA	5%
Total	30%

A reduction in the cost of tin oxide has also been negotiated with one of our suppliers. This will be part of the second phase effort and is not included in the above.

M-1.4.3 Complete the Phase I Portion of the Effort Under Task 2

Phase I portion of Task 2 was completed.

REFERENCES

1. Muirhead, I. and Hawkins, B., Annual Conf. Australian and New Zealand Solar Energy Society – SOLAR '96

2. Jansen, K.W. and Delahoy, A.E. "A Laboratory Technique for the Evaluation of Electrochemical Transparent Conductive Oxide Delamination from Glass Substrates", Thin Solid Films Vol. 423/2, 2003, pp. 153 - 160.

3. Kothandaraman, C., Tonon, T., Huang, C., Delahoy, A.E., "Improvement of a-Si:H P-I-N Devices using Zinc Oxide Based Back-Reflectors", Mat. Res. Soc. Proc., Vol. 219, 1991, pp. 475-480.

REPORT DOCUMENTATION PAGE

Form Approved
OMB NO. 0704-0188

1. AGENCY USE ONLY (Leave blank)	2. REPORT DATE	3. REPORT TYPE AND DATES COVERED
	November 2003	Final Technical Report 1 July 2002–30 June 2003

4. TITLE AND SUBTITLE
Productivity Enhancement for Manufacturing of Amorphous Silicon PV Modules: Final Technical Report, 1 July 2002–30 June 2003

5. FUNDING NUMBERS
PVP4.6101
ZDO-2-30628-14

6. AUTHOR(S)
H. Volltrauer

7. PERFORMING ORGANIZATION NAME(S) AND ADDRESS(ES)
Energy Photovoltaics, Inc.
276 Bakers Basin Road
Lawrenceville, New Jersey 08648

8. PERFORMING ORGANIZATION REPORT NUMBER

9. SPONSORING/MONITORING AGENCY NAME(S) AND ADDRESS(ES)
National Renewable Energy Laboratory
1617 Cole Blvd.
Golden, CO 80401-3393

10. SPONSORING/MONITORING AGENCY REPORT NUMBER
NREL/SR-520-35147

11. SUPPLEMENTARY NOTES
NREL Technical Monitor: R. L. Mitchell

12a. DISTRIBUTION/AVAILABILITY STATEMENT
National Technical Information Service
U.S. Department of Commerce
5285 Port Royal Road
Springfield, VA 22161

12b. DISTRIBUTION CODE

13. ABSTRACT *(Maximum 200 words):* During Phase I, EPV conducted parallel research efforts for achieving higher stabilized module power output through improvements in several manufacturing processing steps, with particular emphasis on the thin-film deposition process. The dual goals of achieving a 10% gain in stabilized output and a 20% reduction in direct costs were accomplished. Early in Phase I, a thorough evaluation of single-junction and tandem amorphous silicon (a-Si) modules was carried out with the goal of determining the best option to use (as a function of application) based on EPV's proprietary batch deposition process. The analysis considered total energy delivery over realistic conditions and the impact on equipment needs and production costs. EPV has concluded that the tandem process is more appropriate for its needs at this time. The overall objective of this subcontract over its two-year duration is to continue the advancement of EPV's a-Si production manufacturing technology and improve the production equipment used in manufacturing. This will allow EPV to reduce module costs by increasing module output, throughput, and yield.

14. SUBJECT TERMS: PV; thin film; deposition process; amorphous silicon (a-Si); devices; tandem module; single junction; maximum power voltage (Vmp); heat aging; shuntbusting process; quantum efficiency;

15. NUMBER OF PAGES

16. PRICE CODE

17. SECURITY CLASSIFICATION OF REPORT	18. SECURITY CLASSIFICATION OF THIS PAGE	19. SECURITY CLASSIFICATION OF ABSTRACT	20. LIMITATION OF ABSTRACT
Unclassified	Unclassified	Unclassified	UL